Author's response to AMT-2020-316: Characterisation and potential for reducing optical resonances in FTIR spectrometers of the …. (NDACC)

Dear Editor,
We would like to thank you for acting as the Editor for our manuscript. We have revised our manuscript carefully taking into account all the comments made by the three referees.

Dear Reviewers,
We would like to thank all of you for your reviews and useful feedback.

Please find below list of responses and revised manuscript including track changes.
(Black: Referee's comments; Blue: Authors' answers)

Best regards
Thomas Blumenstock (on behalf of all co-authors)

Response to comments from Referee 1

Referee:

General Comments.

Good paper.

Thank you very much!

Channel fringes are probably a major source of station-to-station bias within the NDACCIRWG network, especially for weakly-absorbing gases. This is because the amplitude and phase of channel fringes can vary considerably from site to site, even for nominally-identical instruments. So the fringes must either be suppressed, or somehow accounted for in the spectral analysis, or both.

The main deficiency of this manuscript is that the authors provide no explanation of why increasing the wedge angle of the air-gap reduces the amplitude of channel fringes. The central conclusion of the paper is that an 0.8 deg angle for the air-wedge substantially reduces the channeling, as compared with the standard 0.5 deg. But the authors don't tell us why. Ideally, there would be an equation that relates the channel fringe amplitude to the relevant physical properties (reflectivity, flatness, wavenumber, wedge angle). This equation would also explain why the channel fringe amplitudes are so much larger in HgCd than in InSb. Alternatively, there should

be a figure (fringe amplitude versus wedge angle for different wavenumbers) showing the results of computer modelling of the channeling.

Section 2 on the background of the Fabry-Perot effect has been largely extended. Three examples are described in detail: a plane-parallel window at normal and 30° incidence and a wedged plate. Finally, the channeling amplitude as function of wedge angle was calculated and presented in an additional Figure (Fig. 2). These examples illustrate the wavelength dependence as well as the effect of wedging. While the channeling in a plane-parallel plate is not, the reduction by wedging the optical element is wavelength dependent.

In line 95 the authors further state (correctly) that a large tilt suppresses channel fringes, but don't offer any explanation why.

An explanation is added: Wedged optical components avoid channeling because the reflected beams do not superimpose and thus, do not interfere with each other.

Wouldn't anti-reflection coating of the BS and Compensator also decrease the channeling? Explain why this isn't a feasible option?

You're right, in principle an anti-reflection coating on the BS would decrease the channeling. However, such an AR coating is hardly compatible with the broad-band concept of beam splitters used in FTIR spectroscopy. Since the BS is specified for a very large spectral range, for example from 700 to 5000 cm^{-1} for the KBr, such an AR coating would be very complex and would consist of several layers. It is very hard to completely suppress reflections for the entire spectral range without adding any undesirable effects like absorptions or reflections within this muliti-layer coating.

Finally, the authors should discuss potential disadvantages of the larger wedge. For example, might an increased wedge angle between the BS and Compensator cause alignment problems for instruments that are aligned at 1 atm and then operated under vacuum? Or is the air-gap sealed such that the air pressure between the BS and Compensator never changes? Or is there another reason why this doesn't matter?

The air gap is not sealed. In fact, there is a tiny difference in alignment under vacuum. However, this little difference occurs in instruments with small as well as with large BS wedge. So, at least part of this difference has another reason.

The disadvantage of the larger wedge is its incompatibility with other beam splitters. Of course, it is not compatible with pellicle BS used in the FIR spectral domain. Besides this, switching from small to large wedge is quite an effort since two new beam splitters are needed. The KBr BS does not transmit visible light and therefore a second BS (normally CaF_2 or glass) is needed for the alignment procedure by which interference fringes are checked by eye or camera. Furthermore, a full alignment of the spectrometer is needed when switching from small to large wedge. The alignment procedure recommended in NDACC is an effort and described in http://www.acom.ucar.edu/irwg/Griffith_alignment.pptx and https://www.acom.ucar.edu/irwg/HaseBlumenstockAlignment.pdf.

For new instruments switching to a larger wedge is easier since the spectrometer is aligned by the manufacturer. However, a BS with large wedge is not listed in the price list and is available on request only. And the company asks for orders of several items at the same time. At least for new customers or customers from outside the NDACC community this might be hard to know and to order correctly.

Once switched to a pair of beam splitters with increased and matched wedge there is no disadvantage. Of course, the spectrometer needs re-alignment when switching to a larger wedge. This has been done at several sites (Altzomoni, Izaña, Karlsruhe and Kiruna) and is working fine. Switching within this new pair of beam splitters is possible without realignment. The ILS of these instruments is good.

The disadvantages of the larger wedge are discussed in lines 233ff. A few sentences were added here.

Paper should be publishable once these issues (above) are addressed. The authors should also address the more technical problems discussed below.

Specific Comments.

Line 40: "0.9 and 0.11 or 0.23" is ambiguous. I suggest two sentences, one describing air gap periods, and the second discussing the substrate periods.

Done.

Line 45: quantify "significantly"

A sentence is added to quantify the reduction of channeling amplitude with increasing wedge of the air gap.

Line 62: Here you use % as the unit of channel fringe amplitude. Is this a typo? In other places you use ‰. Choose a unit and be consistent.

Done. It was not a typo. We thought % is more appropriate in the introduction to give the magnitude of the effect while ‰ is more appropriate to give the exact numbers in the result section. Anyway, ‰ is used consistently throughout the paper.

Line 98: "design" à "build". It is easy to design an FTS free from channeling; just specify everything to be wedged.

Changed. Well, some devices are difficult to wedge, for example pellicle beam splitters or detector elements. The latter might also cause channeling. Finally, it depends on the wavelength as pointed out in chapter 2. In the NIR spectral domain you're right. In the FIR or even millimeter wave region, however, channel free instruments might be even hard to design.

Line 117: Explain why NDACC uses a set of filters (improve SNR and avoid saturation). This won't be apparent to a non-NDACC reader.

Done.

Line 117: here you use “arc-min” as the wedge angle unit, whereas previously you used degrees. Choose one and use consistently. Or explain why wedge angle requires two different units.

Units were taken from the data sheet of the manufacturer. Changed to degrees.

Line 121: I think that a table would be useful here (or a link to a table) that shows the spectral coverage of each NDACC filter. Also, add a column to Table 2 showing which filters were used at each site.

Done: A column is added to Table 2 and a table of the NDACC filters is added in Appendix A.

Line 130: “…spectral resolution of 0.05 cm^{-1}” is ambiguous. Add the OPD parenthetically.

Done.

Line 148: Figure 2 caption inadequate.

Modified.

Line 170: Move fig.3 earlier, before discussion of fig.4 begins.

Done.

Line 175: I don’t think that the colors add much value to fig.3 since you’ve already told us the correspondence between the three optical cavities and their fringe periods. Perhaps add the HgCd information to fig. 3 and then use colors to denote the detector or the wavenumber of the fitted window.

Done.

Line 185: What about the fringes from the BS substrate? Are these never the largest?

You’re right, there is one case: At Rikubetsu, the substrate of the KBr beam splitter causes the largest channeling amplitude. Fig. 5 has been changed accordingly. For the CaF_2 beam splitter there is no such case (line 185, Fig. 4).

Line 188: Site labels should be identical between figs.4 & 5 (IZ-18 vs IZ-2018)

Done.

Line 197: “The amplitude is even larger as compared to the InSb domain” à “The HgCd amplitudes are larger than those in the InSb domain”. Explain why amplitude is larger in HdCd than in InSb domain?

Done. Is explained in Sect. 2. See also comment and additions to chapter 2.

Lines 200-203: Here you discuss the InSb domain in section 4.2 (HgCdTe Domain). Shouldn’t these sentences be in section 4.1?

Fig. 6 as well as lines 200-203 present and discuss results of the HgCdTe domain. In line 200

(all line numbers refer to original version) 'HgCdTe spectra' was added for clarity.

Line 204: Figure 6 doesn't explain what the three curves are. Are these spectra from different instruments? If so, which ones? Labelling the curves as weak/medium/strong isn't helpful. I can already see with my eyes which one has the strong fringes.

The spectra are taken from different instruments. Labelling of the curves is changed.

The idea of this figure was just to visualize the range of channeling amplitudes within the NDACC network.

Line 208: Mixed units for wedge angles.

Done.

Line 211: "…with far-infrared pellicle…" à"…with unwedged far-infrared pellicle…"

Done.

Line 216: Fig.7 caption. What is the difference between upper and lower panels? Different instruments? If so, which ones? Are the left panels from the same instrument as the right panels? In the lower left panel increasing the wedge from 0.5 to 0.8 deg. caused a factor 3 reduction in the channel fringe amp. But in the lower-right panel, the reduction was much less, perhaps only a factor 1.5. Please discuss.

These measurements were all made with the same instrument. All measurements of Fig. 7 (Fig. 8 in the revised version) were made at Bruker company in Ettlingen. In the first setup, beam splitter with 0.5°, 1.2° and 2.2° were tested (upper panel). The beam splitter was the same for all 3 angles, just different spacers were used.

Since a wedge of 0.8° was chosen for standard beam splitters a test with 0.5° and 0.8° wedge was conducted later on (lower panel). This setup used the same spectrometer as compared to the previous setup (upper panel). The beam splitter is the same for the right and left panel.

Spectra shown in the right and left hand panel show different spectral regions. The channeling amplitudes as well as the reduction factor varies presumably due to wavelength dependent reflectivity of the beam splitter.

Line 218: "To avoid the need for strongly wedged substrates…". This is confusing since the surrounding discussion is about the air-gap fringes. A strongly wedged substrate won't change the air-gap wedge, unless there is an unspoken linkage between the two.

Yes, the strongly wedged substrate won't change the air gap. The idea of line 218 is to make clear that the following paragraph is on air gap fringes only. The discussion before line 218 (line 206-212) is on a special BS with larger wedge of the substrate and of the air gap.

Line 232-233: As in line 218, here you mix the air-gap fringes and the substrate fringes. In my mind these are separate things, with different periods, controlled by different factors. So why would "a larger wedge of the beam slitter substrate" help reduce the air-gap channel fringes?

We agree that a larger wedge of the substrate does not reduce the air gap channel fringes. However, some spectrometer do also show channeling of the substrate. And therefore, in a much earlier attempt to reduce channeling, the air gap and the substrate were strongly wedged at some sites (line 206-212). This chapter is on reducing the channeling of the entire beam splitter not only of the air gap channel. Line 232f is a kind of a summary of chapter 5 highlighting the result of this study that it is possible to manufacture a beam splitter free of 0.11, 0.23 and 0.9 cm^{-1} channel fringes even with a small wedge of the substrate.

Line 234: Perhaps change “incompatibility” to “non-interchangeability”

Done.

Line 248: “Finally, we found that most spectrometers show two dominant channeling frequencies with about 0.1 or 0.2 cm^{-1} and 0.9 cm^{-1} corresponding to beam splitter substrate and beam splitter air gap. In most cases, the channeling caused by the gap of the beam splitter is the leading one. “ à “Finally, we found that most spectrometers show two dominant channeling frequencies with about 0.1 or 0.2 cm^{-1} and 0.9 cm^{-1} corresponding to beam splitter substrate and beam splitter air gap, respectively, the latter usually dominant.”

Done. Thank you for the corrections!

Addition to Sect. 2:

2.1 Fabry-Perot effect in a plane-parallel window at normal incidence

Assume a plane-parallel KBr window of thickness *d* at normal incidence. The refractive index of KBr is 1.5346 at 5 µm and 1.5265 at 10 µm (see https://refractiveindex.info/?shelf=main&book=KBr&page=Li and references therein). We here assume a low finesse, so higher order contributions to the modulated transmission can be neglected. The channeling results from the superposition of the primary transmitted beam with a parasitic beam which is generated by reflection at the exit surface (as result, travelling in the opposite direction as the primary beam) and afterwards at the entrance surface (as result, being redirected again, travelling again parallel to the primary beam). The ratio of intensities between the parasitic and primary beams is given by the Fresnel relation for normal rays:

$$R = \left|\frac{m-1}{m+1}\right|^2 \qquad (2)$$

Here, *m* is the ratio of the refractive indices involved (here, those of KBr and vacuum or air *n_air* = 1.00027 ≈ 1). Because the parasitic ray undergoes two reflections, the intensity ratio is 1.979 ‰ at 5 µm and 1.886 ‰ at 10 µm. This requires that the ratio of the electric amplitudes of the monochromatic electromagnetic waves represented by the two beams is the square root of these values, so 0.0445 at 5 µm and 0.0434 at 10 µm. From a vector addition of the electric amplitudes of the primary and the parasitic ray the peak-to-peak amplitude of the channeling follows: it amounts to a peak-to-peak variation in the intensity of 178 ‰ at 5 µm and 174 ‰ at 10 µm (note that the channeling signal is detected by measuring variable intensities, not wave amplitudes).

The periodicity of the channeling is determined by the requirement that for constructive interference, the path difference between the primary and the parasitic ray needs to equal the extra optical path length travelled by the parasitic ray:

$$2nd = N\lambda \quad (3)$$

Here, n is the refractive index of the plate, λ is the vacuum wavelength, and N is a positive integer number. By rearranging the equation for representation as a function of wavenumbers we find that the fringe period $\Delta\nu$ becomes equidistant as function of wavenumber if the refractive index is constant. If we allow for dispersion $n = n(\nu)$, the channeling period of eq. 1 becomes slightly wavenumber dependent.

$$\Delta\nu = \frac{1}{2n(\nu)d} \quad (4)$$

Note that a resonator formed by a gap instead of KBr will show no (in vacuum) or much less (in laboratory air) variability of the fringe period.

2.2 Fabry-Perot effect in a plane-parallel KBr plate at 30° angle of incidence

Now we investigate a plane-parallel KBr plate of thickness d at 30° angle of incidence, the typical angle in the Bruker FTIR systems. The intensities of the primary and parasitic beams now depend on the state of polarisation. The Fresnel relations for oblique rays provide the reflectivities for linearly polarized waves with the *E* vector oscillating in the plane of incidence (R_p) or perpendicular to it (R_S):

$$R_P = \left|\frac{\cos\beta - m\cos\alpha}{\cos\beta + m\cos\alpha}\right|^2 \quad \text{and} \quad R_S = \left|\frac{\cos\alpha - m\cos\beta}{\cos\alpha + m\cos\beta}\right|^2 \quad (5)$$

Here, α is the incidence angle, while β is the angle with respect to the normal inside the plate. For 30° incidence angle (so $\beta = 19.02°$ at 5 µm and $\beta = 19.12°$ at 10 µm), we calculate the reflectivities as provided in Table 2.

Table 2: Reflectivities calculated from the Fresnel relations

Wavelength [µm]	R_P	R_S
5	0.02845	0.06371
10	0.02768	0.06232

While R_p decreased in comparison to the reflectivity for normal incidence (≈ 0.04), the value of R_S increased. Note that under the Brewster angle, R_p would vanish and channeling caused by the beam splitter (BS) could be removed completely. Operation of a BS near the Brewster angle (here $\approx 57°$) and introduction of a polarizing unit selecting only the perpendicular component for detection would in principle be an alternative approach for removing channeling generated by the BS. However, this would require a complete re-design of the

spectrometer setup (using the BS at a rather inconvenient angle of incidence of nearly 60°) and it would reduce the amount of signal if the source provides unpolarised radiation. (However, the significant polarisation-dependency of the channeling following from the Fresnel equations could be used to prove whether a channeling fringe is created by the BS by using a polarisation filter in front of the detector). Here, if we work with an unpolarised source, we can assume that the channeling amplitude will not be very different from the amplitude estimated for normal incidence.

The period of the channeling fringe as function of wavenumber becomes shorter for geometric reasons when the plate orientation is tilted away from normal incidence: the effective thickness of the BS increases. Note that the change of the channeling period in the presence of dispersion now is created by two mechanisms: the changing relation between optical and geometric path length and the changing angle of transmission:

$$\Delta\nu = \frac{\cos\beta}{2n(\nu)d} \tag{6}$$

2.3 Fabry-Perot effect in a wedged plate

We have seen that there is no significant impact of wavenumber on the channeling amplitude for a plane parallel plate. We will, however, show that a wedge of certain amount is significantly more effective in suppressing channeling at shorter wavelengths.

For our investigation, we assume that the source is incoherent. Therefore, the primary beam can only interfere with the parasitic beam deviated by the wedge (not with a parasitic beam emerging from a different position in the source and exiting the BS under the same angle as the primary beam). As result of the wedge, the wave front of the parasitic beam is now tilted with respect to the primary beam. We analyse the resulting effect on the circular aperture of the collimator focusing the radiation emerging from the interferometer on the exit aperture. The tilt between the outgoing wave fronts of the primary and parasitic plane waves generates equidistant straight stripes of constant phase shift in that plane (stripe orientation perpendicular to wedge). What has been a uniform variation of brightness across the collimator aperture (when either tuning wavelength or plate thickness) now becomes a shift of the stripe pattern perpendicular to the orientation of the stripes. We can estimate the damping effect introduced by the wedge by determining the residual brightness fluctuations emerging from the shifting stripe pattern (technically by integration over the aperture). Obviously, if the stripe pattern becomes denser (larger wedge or shorter wavelength), the brightness fluctuations are further and further reduced. Figure 2 shows the amplitude of the integrated brightness fluctuation as function of cycles across the aperture of the collimator (each cycle is equivalent to adding a detuning of one wavelength across the aperture of the collimator), given by

$$ncycles = \nu D\sin(2\omega) \tag{7}$$

Here, ν is the wavenumber, D the beam diameter, and ω the wedge angle.

Note that our consideration shows that the channeling amplitude is reduced when (1) the aperture of the collimator (or, equivalently, the beam diameter supported by the interferometer) is increased (2) the wavelength is reduced, or (3) the wedge angle is increased.

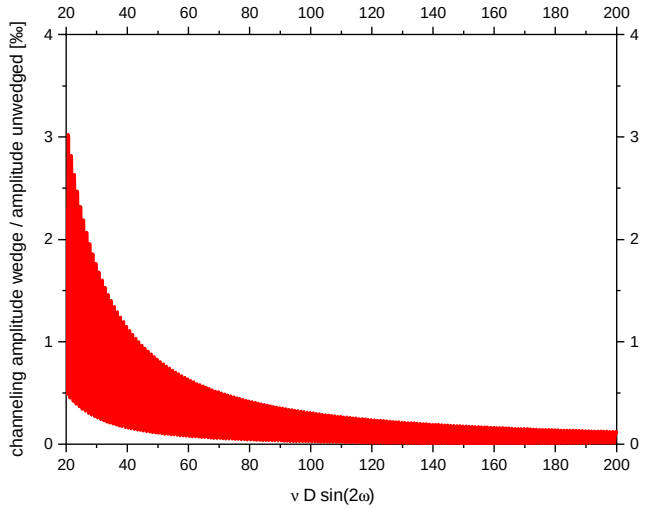

Figure 2: Channeling amplitude as function of wedge angle

Addition 2:

Appendix A

Table A1: List of optical filters used in the IRWG (InfraRed Working Group) of NDACC.

Filter number	Spectral range [µm]	Spectral range [cm^{-1}]	Target species examples
1	2.2 - 2.6	3850 - 4550	HF
2	2.6 - 3.3	3030 - 3850	HCN
3	3.2 - 4.1	2440 - 3130	HCl, CH_4, C_2H_6, HCHO, NO_2
4	3.9 - 5.0	2000 - 2560	N_2O
5	4.6 - 6.3	1590 – 2170	CO, NO, OCS
6	> 7.4	< 1350	O_3, $ClONO_2$, HNO_3, SF_6
7	9.8 – 13.0	770 - 1020	O_3, $ClONO_2$, HNO_3
8	7.5 – 10.2	980 - 1330	O_3

Response to comments from Referee 2 (Dr. Arndt Meier)

Referee:

I wish to congratulate the authors on this well researched and well carried out scientific work.
The manuscript is well and clearly structured, concise, relevant, appropriately illustrated, easy to follow and demonstrates a very good command of the English language.
A pleasure to read.

Thank you very much!

The work presented fits well within the scope of this journal. The work exposes, describes and resolves one of those nagging problems that have been a stone in the shoe of many researchers in this specialist field. The novelty and relevance lies primarily in discussing the issues caused by undesired optical resonances not from the perspective of an individual instrument but on a measurement network wide concise analysis and quantification of the variability and amplitude of these issues and how relevant these are to the overall error budget of trace gases reported by the NDACC (and TCCON) network. The authors include the principal manufacturer of the commonly used spectrometers (Bruker Optics) in the study. This is a good approach and a reflection of decades of good dialogue between cutting edge research and industry to mutual benefit. The authors also discuss and suggest practical technical solutions to the benefit of all affected.

The scientific work has been carried out diligently and the conclusions are sound and relevant. Proper credit is given to past investigations as well as the contributing community who are seemingly all included as co-authors. Abstract and title are appropriate and concise.

Below I have a short list of very minor comments and suggestions that the authors may wish to consider for the final version to improve clarity and readability, but it is nothing that should delay the publication of the final version even if left unconsidered.

- Page 3, section 2, Line 91 "Equation (1) is used to assign..." replace ’assign’ with ’identify’

Done.

- Line 94 correct spelling is "a harmonic" (not an harmonic)

Corrected.

- Line 104, description of Figure 1: Consider adding "where 'l' is denoted 'd' in equation (1)"

Done.

- Line 137 " Then, the background was normalized and a straight line was subtracted using OriginTM software" How was the normalization carried out? Or did the authors mean to say ' Then, the background was normalized by subtracting a straight line (from the laboratory spectra) using OriginTM software'?

Is clarified in the text and in the caption of Fig. 2:
The background was normalized by dividing a straight line that connects the ends of the spectrum using ORIGIN TM software (red line in Fig.2a). The resulting quotient minus 1 (Fig. 2b) was used to perform a FFT analysis.

- page 14, section 5, Line 235 Comment: I wouldn't stress this as an impediment. As long as no pellicle beam splitters are in use, and which seems to be the case for the NDACC (and I believe the TCCON as well) which are the focus of this study, there is no issue as long as the only or at best two beam splitters in use for a given instrument have the same air gap wedge of say 2 degrees. I'm not sure if an additional glass beam splitter is in use for the optical alignment of the FTS, in which case the same wedge would have to be used for that one, too.

Correct, for the standard alignment procedure a second beam splitter (CaF_2 or glass) is needed to observe Haidinger fringes with a telescope. We agree that exclusion of a pellicle beam splitter is not a show stopper for the NDACC and TCCON community, at least when purchasing a new instrument.
New colleagues buying a new instrument might not know this option. For existing instruments, however, switching to beam splitters with larger wedge means an investment of two beam splitters and moreover, a full re-alignment of the spectrometer!

- Line 238: "Such a systematic performance analysis is needed for improving the trace gas retrievals and for calculating complete error budgets." Comment: consider adding "also in order to improve the consistency and quality of the products across the NDACC network"

Done.

- Line 242 Comment: Perhaps a rough indication of typical relative absorption strengths of the weak absorbers listed by the authors would be helpful to put the channeling error amplitudes reported into perspective, possibly earlier in the discussion rather than here.

Added.

- Line 249 Consider replacing "leading one" with "dominating one"

Replaced.

Given that Axel and Denis from Bruker Optics are among the co-authors it would be nice to have And indication (or ideally commitment) that beam splitters with a larger air gap of say 2 degrees are available as an option - if necessary at a small surcharge - for new orders or a modification service for existing beam splitters. That would be great to know even for users outside the NDACC community that may also be affected by channeling in their work.

Agreed. Since recently and as a result of this study the standard air wedge of Bruker beam splitters is 0.8° instead of 0.5°. Beam splitters with an air wedge of 2 degrees are available on request if there is a joint order of a sufficient number of pieces. Up to now this item (beam splitter with 2° air gap) is not included in the price list and is available on request only. A modification service is also available. We agree this option is hard to know for users outside the NDACC community or for newcomers. Therefore, a sentence on availability has been added.

Response to comments from Referee 3

Referee:

This paper describes the problem of optical interferences occurring in FTIR spectrometers that are used in NDACC: it describes some laboratory experiments aiming at identifying and characterising these interferences in about 25 of the NDACC FTIR spectrometers and attributes the interferences to the optical elements inside the spectrometers. It is shown that it is essentially the beamsplitter that causes these interferences. These interferences cause channeling in the spectra that make the observation of weak absorptions in atmospheric spectra difficult. The paper also shows test with beamsplitters with different wedges and concludes that beamsplitters (BS) with a wedge of the gap between the BS and the compensator plate of 0.8_ (instead of the actual standard 0.5_) would be a good choice to minimize the channeling and at the same time avoid re-alignments when exchanging BS.

General comments:
The paper is essentially a technical paper. It is very concise and reads easily; the objectives, methodology and conclusions are clearly formulated. However, being a technical paper, I have the feeling that some technical details are missing, or not clearly spelled out.
- Equation (1) provides the formula for the Free Spectral Range of a Fabry-Pérot (FP) etalon, but it is not mentioned how FSR is calculated for 'a resonator due to both substrates, the beamsplitter and the compensator plate' (line 165).

The formula calculates the resulting frequency out of the cavity length. Here, it is used the other way around. The observed channeling frequency is used to calculate the optical thickness. A channeling frequency of 0.11 cm^{-1} corresponds to 30 mm of KBr which includes beam splitter and compensator plate.

- Tables 3 and 4: at some sites, like Harestua, Garmisch, Altzomoni in Table 3, or Harestua, Zugspitze, Altzomoni in Table 4, some frequencies appear that are very different from the other ones, without any explanation as to their origin: are they due to window effects ? Why are some of these different frequencies classified in Table 2 as the 'standard' F2 or F3 frequencies ?

Yes, this kind of channeling is caused by the detector window.
Line 166f states 'A few spectrometers show an additional channeling fringe with a frequency of about 3 cm^{-1}. This is due to the detector window that is often made of sapphire or calcium fluoride (CaF_2).' And similar in line 193f:
'Two spectrometers show an additional channeling frequency of 2.17 and 3.85 cm^{-1}, indicating that the wedge of the detector window is not sufficient in these cases.'
We added the site names to clarify this.

Please also note the color code in Figs. 4 and 5 to indicate the origin of the channeling with the largest amplitude at each site.

Table 2 or 3 (We guess you refer to Table 3):
If the standard F2 or F3 frequency was not observed other frequencies moved forward (Toronto, Harestua, Garmisch, Zugspitze and Altzomoni).

- In Table 4, A4 (= 21 pro mille) at Ny Alesund corresponds to F4 . Why is this amplitude included in the range of amplitudes of the channeling caused by the gap of the BS, with frequency F1 = 0.9 cm^{-1}) ?

Yes, F4 (2.17 cm^{-1}) is attributed to an optical window, for example the detector window, see line 193-194. Also in Fig. 5 color code denotes F4 as caused by a window (in blue) not the gap of the BS.

The range covers the entire range observed not only due to BS channeling. For clarity, the sequence of sentences has been changed in line 195f: Instead of 'Figure 5 shows the amplitude of the strongest channeling frequency of each spectrometer. In most cases, channeling caused by the gap of the beam splitter is the most pronounced one. The amplitudes range from 0.3 to 21 ‰ with …' has been changed to 'Figure 5 shows the amplitude of the strongest channeling frequency of each spectrometer. The amplitudes range from 0.3 to 21 ‰ with … . In most cases, channeling caused by the gap of the beam splitter is the most pronounced one.'
And similar in line 170-172.

- In Table 4: why at Lauder, 2 different frequencies are assigned to F1 ? The same question holds for a few other sites and other frequencies (F2) in Table 4.

If the FFT analysis yields channeling at two frequencies close to each other the corresponding amplitudes were listed in the same column. You're right, for Lauder the second frequency in the F1 column does not fit here. It is changed in Table 4.

Specific comments:
- Line 49: I would specify 'total and partial column abundances' instead of simply 'column abundances'

Done.

- Line 93-94: The sentence is erroneous as it is formulated here. I suggest to replace it as follows: "The Fabry-Pérot etalons generated by these optical components have rather low etendu and therefore the undesired parasitic effects caused in their spectral transmission is well described as an harmonic oscillation." I believe that this is what the authors intend to say. It would also be good to give the definition of 'etendu of a FP' here, or to add a reference to a definition.

Sentence is corrected as suggested. Thanks for pointing to this paragraph and we also found a mix-up of terminology: we intended to refer to the finesse of the resonator here, not to the etendue. The low reflectivity yields a low finesse. The finesse is a measure of the number of reflections within a cavity and a low reflectivity means a low finesse and small number of reflections within the cavity.

- Table 1: Apparently the FSR given in the table assumes theta = 0_. However, in the standard NDACC FTIR spectrometer configuration, theta is typically 45_ for the beamsplitter. So I am confused: how has the experiment been set up exactly ?

You're right, the FSR given in the table is calculated with theta = 0. In the NDACC FTIR spectrometer configuration theta is 30°. However, due to refraction theta is smaller inside the beam splitter. According to Snell's law theta is 19° for n=1.5. *Cos* 19° is about 0.95 and therefore close to 1.0.

- Line 117: It is stated that NDACC filters with a wedge of 10', if properly oriented, do not cause channeling. Don't they cause any channeling at all, or are the frequencies of the channeling such that they don't disturb significantly the retrieval of typical NDACC atmospheric spectra ?

If the wedge is sufficient they don't cause any channeling at all. The reflecting beams do not overlap and thus do not interfere with each other.

- Figure 2: Why has the x-axis been given in 1/Frequency whereas Figure 3 has an x-axis in frequency ?

In the OriginTM software the inverse FFT has been applied which calculates the results as function of 1/frequency as shown in Fig. 2. For the presentation and discussion of the results the results were given in terms of frequency to be consistent with the spectra shown in Figs. 6 and 7.

The paper deserves being published, after some revisions to cope with the above comments.

Characterisation and potential for reducing optical resonances in FTIR spectrometers of the Network for the Detection of Atmospheric Composition Change (NDACC)

Thomas Blumenstock[1], Frank Hase[1], Axel Keens[2], Denis Czurlok[2], Orfeo Colebatch[3], Omaira Garcia[4], David W. T. Griffith[5], Michel Grutter[6], James W. Hannigan[7], Pauli Heikkinen[8], Pascal Jeseck[9], Nicholas Jones[5], Rigel Kivi[8], Erik Lutsch[3], Maria Makarova[10], Hamud Kh. Imhasin[10], Johan Mellqvist[11], Isamu Morino[12], Tomoo Nagahama[13], Justus Notholt[14], Ivan Ortega[7], Mathias Palm[14], Uwe Raffalski[15], Markus Rettinger[16], John Robinson[17], Matthias Schneider[1], Christian Servais[18], Dan Smale[17], Wolfgang Stremme[6], Kimberly Strong[3], Ralf Sussmann[16], Yao Té[9], Voltaire A. Velazco[5]

[1]Karlsruhe Institute of Technology (KIT), Institute of Meteorology and Climate Research (IMK-ASF), Karlsruhe, Germany
[2]Bruker Optics GmbH, Ettlingen, Germany
[3]Department of Physics, University of Toronto, Toronto, Canada
[4]Izaña Atmospheric Research Centre (IARC), Meteorological State Agency of Spain (AEMET), Tenerife, Spain
[5]Centre for Atmospheric Chemistry, University of Wollongong, Wollongong, Australia
[6]Centro de Ciencias de la Atmósfera, Universidad Nacional Autónoma de México (UNAM), Mexico City, México
[7]National Center for Atmospheric Research (NCAR), Boulder, CO, USA
[8]Finnish Meteorological Institute (FMI), Sodankylä, Finland
[9]Laboratoire d'Etudes du Rayonnement et de la Matière en Astrophysique et Atmosphères (LERMA-IPSL), Sorbonne Université, CNRS, Observatoire de Paris, PSL Université, 75005 Paris, France
[10]Saint Petersburg State University, Atmospheric Physics Department, St. Petersburg, Russia
[11]Department of Earth and Space Science, Chalmers University of Technology, Göteborg, Sweden
[12]National Institute for Environmental Studies (NIES), Tsukuba, Ibaraki 305-8506, Japan
[13]Institute for Space-Earth Environmental Research (ISEE), Nagoya University, Nagoya, Japan
[14]Institute of Environmental Physics, University of Bremen, Bremen, Germany
[15]Swedish Institute of Space Physics (IRF), Kiruna, Sweden
[16]Karlsruhe Institute of Technology, IMK-IFU, Garmisch-Partenkirchen, Germany
[17]National Institute of Water and Atmospheric Research Ltd (NIWA), Lauder, New Zealand
[18]Institut d'Astrophysique et de Géophysique, Université de Liège, Liège, Belgium

Correspondence to: Thomas Blumenstock (thomas.blumenstock@kit.edu)

Abstract. Although optical components in Fourier transform infrared (FTIR) spectrometers are preferably wedged, in practice, infrared spectra typically suffer from the effects of optical resonances ("channeling") affecting the retrieval of weakly absorbing gases. This study investigates the level of channeling of each FTIR spectrometer within the Network for the Detection of Atmospheric Composition Change (NDACC). Dedicated spectra were recorded by more than twenty NDACC FTIR spectrometers using a laboratory mid-infrared source and two detectors. In the InSb detector domain (1900 – 5000 cm^{-1}), we find that the amplitude of the most pronounced channeling frequency amounts to 0.1 to 2.0 ‰ of the spectral background level, with a mean of (0.68 ± 0.48) ‰ and a median of 0.60 ‰. In the HgCdTe detector domain (700 – 1300 cm^{-1}), we find even stronger effects, with the largest amplitude ranging from 0.3 to 21 ‰ with a mean of (2.45 ± 4.50) ‰ and a median of

1.2 ‰. For both detectors, the leading channeling frequencies are 0.9 and 0.11 or 0.23 cm^{-1} in most spectrometers. These observed spectral frequencies of 0.11 and 0.23 cm^{-1} correspond to the optical thickness of the beam splitter substrate. The 0.9 cm^{-1} channeling is caused by the air gap in between the beam splitter and compensator plate. ~~(0.9 cm^{-1}) and the beam splitter substrate itself (0.11 and 0.23 cm^{-1})~~. Since the air gap is a significant source of channeling and the corresponding amplitude differs strongly between spectrometers, we propose new beam splitters with the wedge of the air gap increased to at least 0.8°. We tested the insertion of spacers in a beam splitter's air gap to demonstrate that increasing the wedge of the air gap decreases the 0.9 cm^{-1} channeling amplitude significantly. A wedge of the the air gap of 0.8° reduces the channeling amplitude by about 50% while a wedge of about 2° removes the 0.9 cm^{-1} channeling completely. This study shows the potential for reducing channeling in the FTIR spectrometers operated by the NDACC, thereby increasing the quality of recorded spectra across the network.

1 Introduction

Ground-based FTIR (Fourier transform infrared) spectroscopy is a widely used technique for measuring total and partial column abundances of a variety of trace gases in the atmosphere. Within the Network for the Detection of Atmospheric Composition Change (NDACC), this technique is used at about twenty sites covering a wide range of geographical latitudes. The NDACC data are used to study short and long-term variability of the atmosphere as well as for satellite data validation (De Mazière et al., 2018). For both applications, high data quality and station-to-station consistency are of utmost importance. Ground-based FTIR spectroscopy provides data of high quality (e.g. Schneider and Hase, 2008). However, several key instrumental characteristics need to be addressed. These parameters such as detector non-linearity (Abrams et al., 1994), instrumental line shape (ILS; Hase et al., 1999), intensity fluctuations (Keppel-Aleks et al., 2007), precise solar tracking (Gisi et al., 2011), and sampling error (Messerschmidt et al., 2010; Dohe et al., 2013) have been studied in some detail and need to be taken into account.

In this paper, channeling – the presence of instrument-induced periodic oscillations of spectral transmission resulting from internal optical resonances – will be investigated and discussed. In the past, each site or each new spectrometer was tested for channeling individually. This paper describes a network-wide exercise for characterizing channeling in FTIR spectrometers. Channeling is caused by interference of reflections of the incoming light at parallel transmitting surfaces of optical elements. In practice, the resulting channeling amplitudes are less than 10 ‰~~%~~ in signal. Thus, the retrieved data for species with strong absorption signatures, as for example ozone and many others, are less critically affected. However, the retrieved trace gas amounts of weak absorbers can be substantially disturbed. In such cases, channeling becomes an important component of the total error budget.

Recently, time series of column abundances of formaldehyde (HCHO) were retrieved from NDACC FTIR sites (Vigouroux et al., 2018, 2020). The studies of Vigouroux also includes an error characterisation of the HCHO product. Within the network, two retrieval codes are in use: SFIT4 and PROFFIT. While the retrieval codes were inter-compared and show consistent results

(Hase et al., 2004), the assumed error budgets differ slightly. The stations using PROFFIT include an error contribution due to channeling while the stations using SFIT4 do not. The result is a larger total error for HCHO data retrieved with PROFFIT as compared to SFIT4 (Vigouroux et al., 2018). In the PROFFIT error calculation, a set of typical channeling frequencies and amplitudes is taken into account. More specifically, channeling amplitudes of 0.5 ‰ for four frequencies are assumed: 0.005, 0.2, 1.0, and 3.0 cm^{-1}. The resulting error contribution doubles the total error of HCHO columns amounts.

In order to make this assumption more robust and to quantify more carefully the differences from spectrometer to spectrometer, an exercise was performed to measure channeling frequencies and amplitudes of NDACC FTIR spectrometers. Since atmospheric spectra are densely populated with absorption signatures interfering with the signal generated by channeling; the test was designed using spectra collected in a laboratory setting. Section 2 briefly describes the origin of channeling, Sect. 3 the setup of this exercise, and Sect. 4 shows the results followed by a discussion. Finally, to reduce the channeling amplitude, the investigation of a modified beam splitter design is presented in Sect. 5, and lastly, Sect. 6 gives the conclusions.

2 Spectral transmission of a Fabry-Perot cavity

In an FTIR spectrometer, the transmitted light passes through several optical components such as optical windows, optical filters and a beam splitter, typically comprised of a beam-splitting layer system deposited on a transparent substrate and a compensator. At the transmitting surfaces of these components, the optical beam is partially reflected. In the case of parallel surfaces, each pair of surfaces defines a cavity (Fig. 1a) in which multiple reflections occur. Due to interference of the reflected light, a standing wave is created (Fig. 1b). This effect is called the Fabry-Perot or etalon effect or channeling. The optical length of the cavity defines the free spectral range $\nu_{(FSR)}$ as

$$\nu(FSR) = 1/(2ndcos\theta) \quad (1)$$

with n refractive index and d thickness of the optical component (Hecht, 2017). θ is the angle between incoming light beam and the normal of the optical surface (Fig. 1a). Equation (1) is used to identify~~assign~~ the optical element responsible for a certain channeling frequency. Table 1 gives a few examples of $\nu_{(FSR)}$ for optical materials commonly used in FTIR spectrometers.

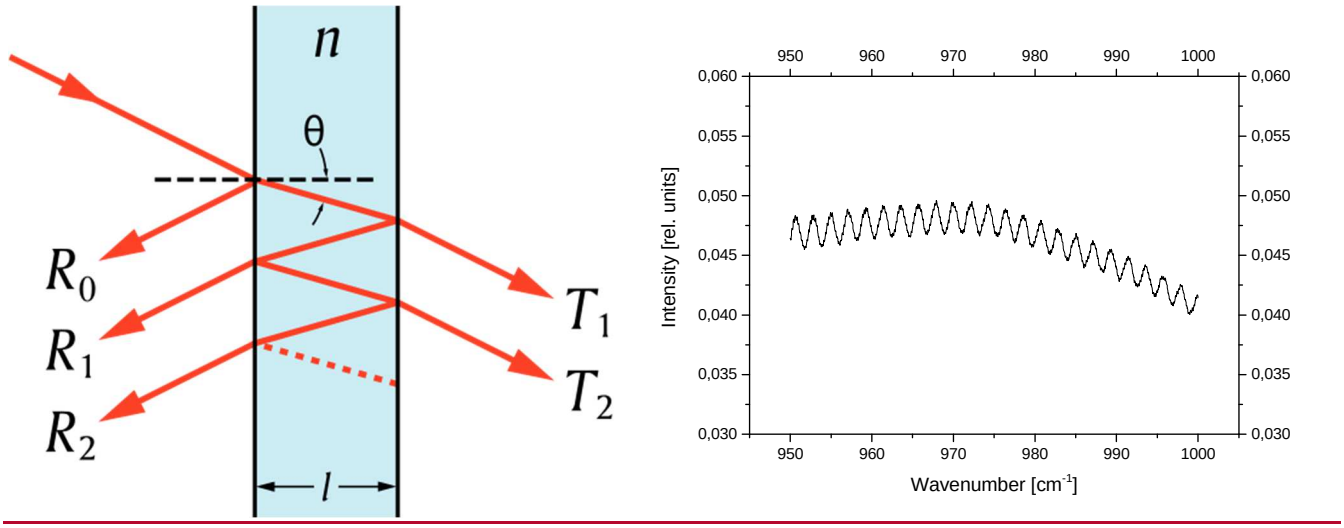

Figure 1: (a) Multiple reflections at parallel surfaces in an optical component where '*l*' is denoted '*d*' in equation (1) (taken from Wikimedia Commons: https://commons.wikimedia.org/), (b) Channeling in an IR spectrum.

Table 1: Free spectral range $\nu_{(FSR)}$ of some components typically used in NDACC FTIR spectrometers with $\cos\theta = 1$.

Material	used as	*n*	*d* [mm]	$\nu_{(FSR)}$ [cm^{-1}]
Air	Gap in between beam splitter and compensator plate	1	5.5	0.91
KBr	Beam splitter substrate	1.5	15	0.22
CaF_2	Beam splitter substrate	1.4	15	0.24
CaF_2	Detector window	1.4	1.0	3.57
Ge	Detector window	4.4	1.0	1.14
KRS-5 (TlBr-TlI)	Detector window	2.37	1.0	2.11
Sapphire	Detector window	1.65	1.0	3.0
ZnSe	Detector window	2.2	1.0	2.27

~~The Fabry Perot etalons generated by these undesired parasitic effects naturally have rather low etendue, so the resulting spectral transmission is well described by assuming an harmonic oscillation.~~ The Fabry-Pérot etalons generated by these optical components have rather low reflectivity and therefore the undesired parasitic effects caused in their spectral transmission is well described as a harmonic oscillation.

For demonstrating the plausibility of our empirical experimental results, we here provide some basic considerations concerning the channeling effects created by a Fabry-Perot etalon of low finesse. Further background information can be found in Ismail et al., (2016) and references herein.

2.1 Fabry-Perot effect in a plane-parallel window at normal incidence

Assume a plane-parallel KBr window of thickness d at normal incidence. The refractive index of KBr is 1.5346 at 5 µm and 1.5265 at 10 µm (see https://refractiveindex.info/?shelf=main&book=KBr&page=Li and references therein). We here assume a low finesse, so higher order contributions to the modulated transmission can be neglected. The channeling results from the superposition of the primary transmitted beam with a parasitic beam which is generated by reflection at the exit surface (as result, travelling in the opposite direction as the primary beam) and afterwards at the entrance surface (as result, being redirected again, travelling again parallel to the primary beam). The ratio of intensities between the parasitic and primary beams is given by the Fresnel relation for normal rays:

$$R = \left|\frac{m-1}{m+1}\right|^2 \quad (2)$$

Here, m is the ratio of the refractive indices involved (here, those of KBr and vacuum or air n_{air} = 1.00027 ≈ 1). Because the parasitic ray undergoes two reflections, the intensity ratio is 1.979 ‰ at 5 µm and 1.886 ‰ at 10 µm. This requires that the ratio of the electric amplitudes of the monochromatic electromagnetic waves represented by the two beams is the square root of these values, so 0.0445 at 5 µm and 0.0434 at 10 µm. From a vector addition of the electric amplitudes of the primary and the parasitic ray the peak-to-peak amplitude of the channeling follows: it amounts to a peak-to-peak variation in the intensity of 178 ‰ at 5 µm and 174 ‰ at 10 µm (note that the channeling signal is detected by measuring variable intensities, not wave amplitudes).

The periodicity of the channeling is determined by the requirement that for constructive interference, the path difference between the primary and the parasitic ray needs to equal the extra optical path length travelled by the parasitic ray:

$$2nd = N\lambda \quad (3)$$

Here, n is the refractive index of the plate, λ is the vacuum wavelength, and N is a positive integer number. By rearranging the equation for representation as a function of wavenumbers we find that the fringe period $\Delta\nu$ becomes equidistant as function of wavenumber if the refractive index is constant. If we allow for dispersion $n = n(\nu)$, the channeling period of eq. 1 becomes slightly wavenumber dependent.

$$\Delta\nu = \frac{1}{2n(\nu)d} \quad (4)$$

Note that a resonator formed by a gap instead of KBr will show no (in vacuum) or much less (in laboratory air) variability of the fringe period.

2.2 Fabry-Perot effect in a plane-parallel KBr plate at 30° angle of incidence

Now we investigate a plane-parallel KBr plate of thickness d at 30° angle of incidence, the typical angle in the Bruker FTIR systems. The intensities of the primary and parasitic beams now depend on the state of polarisation. The Fresnel relations for oblique rays provide the reflectivities for linearly polarized waves with the E vector oscillating in the plane of incidence (R_p) or perpendicular to it (R_S):

$$R_P = \left|\frac{\cos\beta - m\cos\alpha}{\cos\beta + m\cos\alpha}\right|^2 \quad \text{and} \quad R_S = \left|\frac{\cos\alpha - m\cos\beta}{\cos\alpha + m\cos\beta}\right|^2 \quad (5)$$

Here, α is the incidence angle, while β is the angle with respect to the normal inside the plate. For 30° incidence angle (so $\beta = 19.02°$ at 5 µm and $\beta = 19.12°$ at 10 µm), we calculate the reflectivities as provided in Table 2.

Table 2: Reflectivities calculated from the Fresnel relations

Wavelength [µm]	R_P	R_S
5	0.02845	0.06371
10	0.02768	0.06232

While R_p decreased in comparison to the reflectivity for normal incidence (≈ 0.04), the value of R_S increased. Note that under the Brewster angle, R_p would vanish and channeling caused by the beam splitter (BS) could be removed completely. Operation of a BS near the Brewster angle (here $\approx 57°$) and introduction of a polarizing unit selecting only the perpendicular component for detection would in principle be an alternative approach for removing channeling generated by the BS. However, this would require a complete re-design of the spectrometer setup (using the BS at a rather inconvenient angle of incidence of nearly 60°) and it would reduce the amount of signal if the source provides unpolarised radiation. (However, the significant polarisation-dependency of the channeling following from the Fresnel equations could be used to prove whether a channeling fringe is created by the BS by using a polarisation filter in front of the detector). Here, if we work with an unpolarised source, we can assume that the channeling amplitude will not be very different from the amplitude estimated for normal incidence.

The period of the channeling fringe as function of wavenumber becomes shorter for geometric reasons when the plate orientation is tilted away from normal incidence: the effective thickness of the BS increases. Note that the change of the channeling period in the presence of dispersion now is created by two mechanisms: the changing relation between optical and geometric path length and the changing angle of transmission:

$$\Delta\nu = \frac{\cos\beta}{2n(\nu)d} \quad (6)$$

2.3 Fabry-Perot effect in a wedged plate

We have seen that there is no significant impact of wavenumber on the channeling amplitude for a plane parallel plate. We will, however, show that a wedge of certain amount is significantly more effective in suppressing channeling at shorter wavelengths.

For our investigation, we assume that the source is incoherent. Therefore, the primary beam can only interfere with the parasitic beam deviated by the wedge (not with a parasitic beam emerging from a different position in the source and exiting the BS under the same angle as the primary beam). As result of the wedge, the wave front of the parasitic beam is now tilted with respect to the primary beam. We analyse the resulting effect on the circular aperture of the collimator focusing the radiation emerging from the interferometer on the exit aperture. The tilt between the outgoing wave fronts of the primary and parasitic plane waves generates equidistant straight stripes of constant phase shift in that plane (stripe orientation perpendicular to wedge). What has been a uniform variation of brightness across the collimator aperture (when either tuning wavelength or plate thickness) now becomes a shift of the stripe pattern perpendicular to the orientation of the stripes. We can estimate the damping effect introduced by the wedge by determining the residual brightness fluctuations emerging from the shifting stripe pattern (technically by integration over the aperture). Obviously, if the stripe pattern becomes denser (larger wedge or shorter wavelength), the brightness fluctuations are further and further reduced. Figure 2 shows the amplitude of the integrated brightness fluctuation as function of cycles across the aperture of the collimator (each cycle is equivalent to adding a detuning of one wavelength across the aperture of the collimator), given by

$$ncycles = \nu D\sin(2\omega) \quad (7)$$

Here, ν is the wavenumber, D the beam diameter, and ω the wedge angle.

Note that our consideration shows that the channeling amplitude is reduced when (1) the aperture of the collimator (or, equivalently, the beam diameter supported by the interferometer) is increased (2) the wavelength is reduced, or (3) the wedge angle is increased.

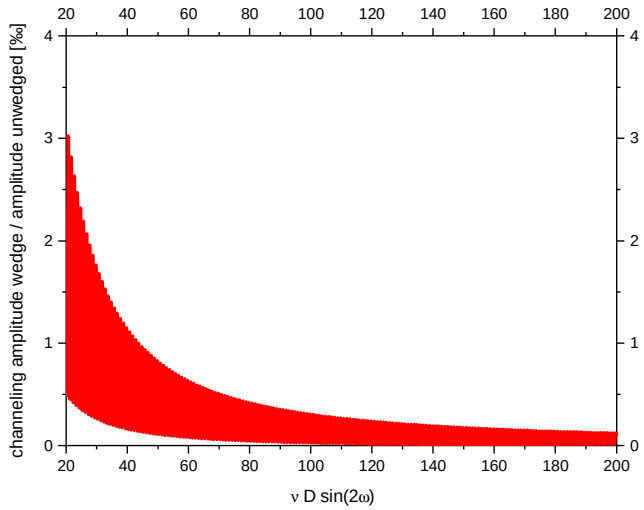

Figure 2: Channeling amplitude as function of wedge angle

While a Fabry-Pérot spectrometer is designed and aligned such that the surfaces are parallel to build a cavity, an FTIR spectrometer is designed differently: In order to reduce or avoid channeling, optical components need to be wedged or installed with a large tilt. A large tilt is not feasible in many cases. Thus, optical components are normally wedged. As shown in this section wedged optical components reduce channeling because the reflected beams do not superimpose and thus, do not interfere with each other. These wedged components require a special design and limits compatibility with non-wedged devices. Furthermore, some components such as detector elements are not available as wedged versions (the partially transparent detector element can also act as optical cavity). Therefore, in practice it is challenging to build an FTIR spectrometer that is completely free of channeling. ~~**In order to reduce or avoid channeling, optical components need to be wedged or installed with a large tilt. A large tilt is not feasible in many cases. Thus, components are normally wedged, which requires a special design and limits compatibility with non-wedged devices. Furthermore, some components such as detector elements are not available as wedged versions (the partially transparent detector element can also act as optical cavity). Therefore, in practice it is challenging to design an FTIR spectrometer that is completely free of channeling.**~~

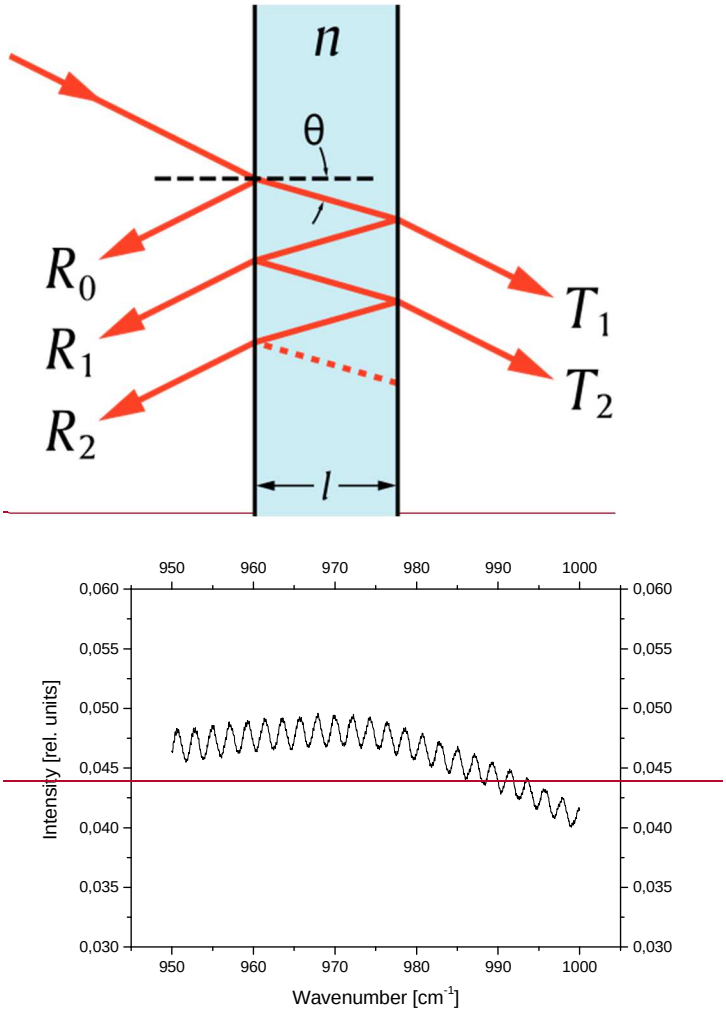

~~**Figure 1: (a) Multiple reflections at parallel surfaces in an optical component (taken from Wikimedia Commons: https://commons.wikimedia.org/), (b) Channeling in an IR spectrum.**~~

~~**Table 1: Free spectral range $\nu_{(FSR)}$ of some components typically used in NDACC FTIR spectrometers.**~~

~~Material~~	~~used as~~	~~*n*~~	~~*d* [mm]~~	~~$\nu_{(FSR)}$ [cm^{-1}]~~
~~Air~~	~~Gap in between beam splitter and compensator plate~~	~~1~~	~~5.5~~	~~0.91~~

KBr	Beam splitter substrate	1.5	15	0.22
CaF_2	Beam splitter substrate	1.4	15	0.24
CaF_2	Detector window	1.4	1.0	3.57
Ge	Detector window	4.4	1.0	1.14
KRS-5 (TlBr-TlI)	Detector window	2.37	1.0	2.11
Sapphire	Detector window	1.65	1.0	3.0
ZnSe	Detector window	2.2	1.0	2.27

3 Channeling test exercise

3.1 Experimental setup

In atmospheric spectra, channeling can be difficult to see due to the presence of complex atmospheric signatures. Therefore, laboratory spectra are used for this exercise, recorded either with a mid-infrared globar or with a black body of at least 1000 °C temperature. Since these types of sources do not include a window, no additional channeling is added to the spectra. A temperature of 1000 °C is required to record spectra with a sufficient signal-to-noise ratio in a reasonable amount of time.

Within NDACC, two detectors and the NDACC filter set are used (Table A1). The optical filters are used to increase the signal to noise ratio of the spectra. The NDACC filters have a wedge of 0.17°~~10 arc min~~ and therefore, if properly oriented, do not cause channeling. Therefore, not all filters but both detectors were included in this exercise. More specifically, NDACC filter #3 (2400 to 3000 cm^{-1} spectral range) for the InSb detector and NDACC filter #6 (700 to 1300 cm^{-1} spectral range) for the HgCdTe detector were used. Some sites (Harestua, Paris, Wollongong, and Lauder_120HR) use filter #7 (700 to 1000 cm^{-1} spectral range) and #8 (1000 to 1400 cm^{-1} spectral range) instead of filter #6 (Table 3). In this case, filter #7 was used for this exercise. Filter #3 was selected since this filter range is used for the retrieval of HCHO column abundances.

Multiple reflections within optical components such as optical windows or beam splitters typically show channeling frequencies of a few tenths of a wavenumber up to a few wavenumbers. In general, higher frequency channeling with wavenumbers below 0.1 cm^{-1} might occur when different optical components form the surfaces of the resulting cavity, e.g. in the Bruker 120HR spectrometer the rim of the entrance field stop is part of a resonator of about 1 m length. However, this is seldom the case in an FTIR spectrometer and secondly, due to the high frequency, easily detectable even in atmospheric spectra.

In order to focus on channeling due to multiple reflections inside optical components and to achieve a very good signal-to-noise ratio, a spectral resolution of 0.05 cm^{-1} (OPD = 180 cm) was chosen. This resolution allowed us to add thousand

interferograms within a few hours, thereby achieving signal-to-noise ratio that allowed channeling amplitudes to be detected and quantified on a per mille scale.

3.2 Analysis of channeling test spectra

To quantify channeling frequencies and their amplitudes, an FFT (Fast Fourier Transform) analysis of the spectra was conducted. First of all, a spectral interval was chosen with a nearly constant intensity: 950 to 1000 cm^{-1} for HgCdTe and 2550 to 2600 cm^{-1} for InSb spectra. This step was carried out using OPUS™, a software package from Bruker Optics to control FTIR spectrometers (Fig. 32a). Then, the background was normalized ~~and a straight line was subtracted using Origin™ software (Fig. 2b).~~ by dividing a straight line that connects the ends of the spectrum using ORIGIN™ software (red line in Fig.3a). The quotient minus 1 is the basis for the FFT analysis (Fig. 3b). Finally, an inverse FFT was conducted also with Origin™ software (Fig. 32c).

(a)

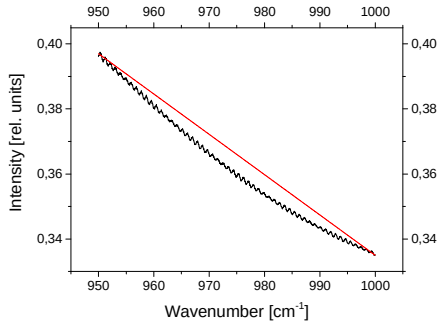

(b)

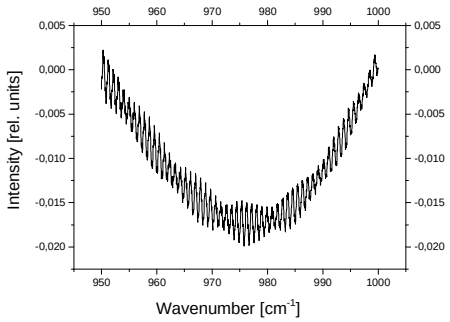

(c)

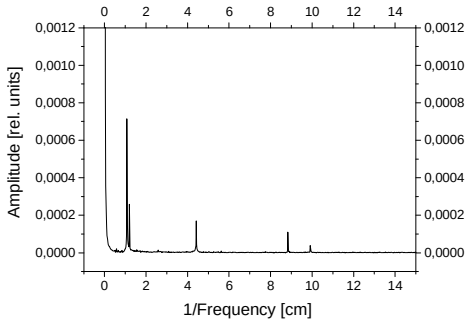

Figure ~~2~~3: Analysis of a channeling test spectrum: (a) Cut off a window of 50 cm^{-1}; a straight line is calculated that connects the ends of the spectrum (red line); (b) Normalize background by dividing this straight line and subtract a constant of 1~~straight line~~; (c) Result of FFT analysis

4 Results and Discussion

In this section, the results are presented for more than twenty spectrometers. Table 3~~2~~ provides the list of spectrometers included in this study. Please note that a few spectrometers do not include an HgCdTe detector: Garmisch, Karlsruhe, and Sodankylä.

Table ~~2~~3: List of spectrometers contributing to the channeling test exercise, sorted by latitude of the site, from north (Eureka) to south (Arrival Heights).

Site	Acronym	Type	Beam splitter setup	Optical filter	Team
Eureka	EUR	Bruker 125 HR	KBr	#3 & #6	U Toronto
Ny-Ålesund	NY	Bruker 120/5 HR	KBr for HgCdTe, CaF_2 for InSb det.	#3 & #6	U Bremen
Thule	THU	Bruker 125 HR	KBr	#3	NCAR
Kiruna	KIR	Bruker 120/5 HR	KBr	#3 & #6	KIT-ASF, IRF
Sodankylä	SOD	Bruker 125 HR	CaF_2, no HgCdTe det.	#3	FMI
Harestua	HAR	Bruker 120 M	KBr	#3 & #8	U Gothenborg
St. Petersburg	STP	Bruker 120 HR	KBr	Ind. #3 & #6	SPbU
Bremen	BRE	Bruker 125 HR	KBr	#3 & #6	U Bremen
Karlsruhe	KAR	Bruker 125 HR	CaF_2, no HgCdTe det.	#3	KIT-ASF
Paris	PAR	Bruker 125 HR	KBr for HgCdTe, CaF_2 for InSb det.	Ind. #3 & #7	Sorbonne U
Garmisch	GAR	Bruker 125 HR	CaF_2, no HgCdTe det.	#3	KIT-IFU
Zugspitze	ZUG	Bruker 120/5 HR	KBr	#3 & #6	KIT-IFU

Jungfraujoch	JJO	Bruker 120 HR	KBr	#3 & #6	U Liège
Toronto	TOR	BOMEM DA8	KBr	#3 & #6	U Toronto
Rikubetsu	RIK	Bruker 120/5 HR	KBr for HgCdTe, CaF_2 for InSb det.	#3 & #6	U Nagoya, NIES
Boulder	BOU	Bruker 120/5 HR	KBr	#3	NCAR
Tsukuba	TSU	Bruker 125 HR	KBr for HgCdTe, CaF_2 for InSb det.	#3 & #6	NIES
Izaña	IZ	Bruker 120/5 HR	KBr	#3 & #6	AEMet, KIT-ASF
Mauna Loa	MLO	Bruker 120/5 HR	KBr	#3 & #6	NCAR
Altzomoni	ALT	Bruker 120/5 HR	KBr	#3 & #6	UNAM
Wollongong	WOL	Bruker 125 HR	KBr	#3 & #7	U Wollongong
Lauder	LAU	Bruker 120 HR ~~&~~ Bruker 125 HR	KBr KBr	#3 & #7 #3 & #6	NIWA
Arrival Heights	AH	Bruker 125 HR	KBr	#3 & #6	NIWA

These sites primarily serve the TCCON (Total Carbon Column Observing Network; Wunch et al., 2010) and just contribute with InSb spectra to NDACC and to this exercise. These spectrometers use a CaF_2 beam splitter instead of KBr; the latter is normally used in NDACC for enabling measurements in the HgCdTe spectral range. Ny-Ålesund, Paris, Rikubetsu and Tsukuba sites use a CaF_2 beam splitter for InSb and a KBr beam splitter for HgCdTe measurements. Tables ~~3~~4 and 5~~4~~ list the detected channeling frequencies and their amplitudes in spectra recorded with InSb and HgCdTe detectors, respectively.

4.1 InSb detector domain

Figure ~~3~~4 shows the detected channeling frequencies and their amplitudes in InSb spectra analysed at about 2600 cm^{-1}. Most spectrometers show the expected channeling frequencies: about 0.9 cm^{-1} and 0.11 or 0.23 cm^{-1}. These frequencies are consistent with (i) the gap between beam splitter and compensator plate (0.9 cm^{-1}), and (ii) the beam splitter substrate (0.23 cm^{-1}; Table 1). A frequency of 0.11 cm^{-1} corresponds to a resonator due to both substrates, the beam splitter and the compensator plate.

A few spectrometers (Harestua, Garmisch, Toronto, Boulder and Izaña-2018) show an additional channeling fringe with a frequency of about 3 cm^{-1}. This is due to the detector window that is often made of sapphire or calcium fluoride (CaF_2). Also in Izaña, this channeling frequency was detected in 2018. In December 2018, the detector was exchanged because of decreasing sensitivity. The new detector (Izaña-2019) shows much less channeling. Detectors purchased in the 1990s sometimes had a detector window with insufficient wedge.

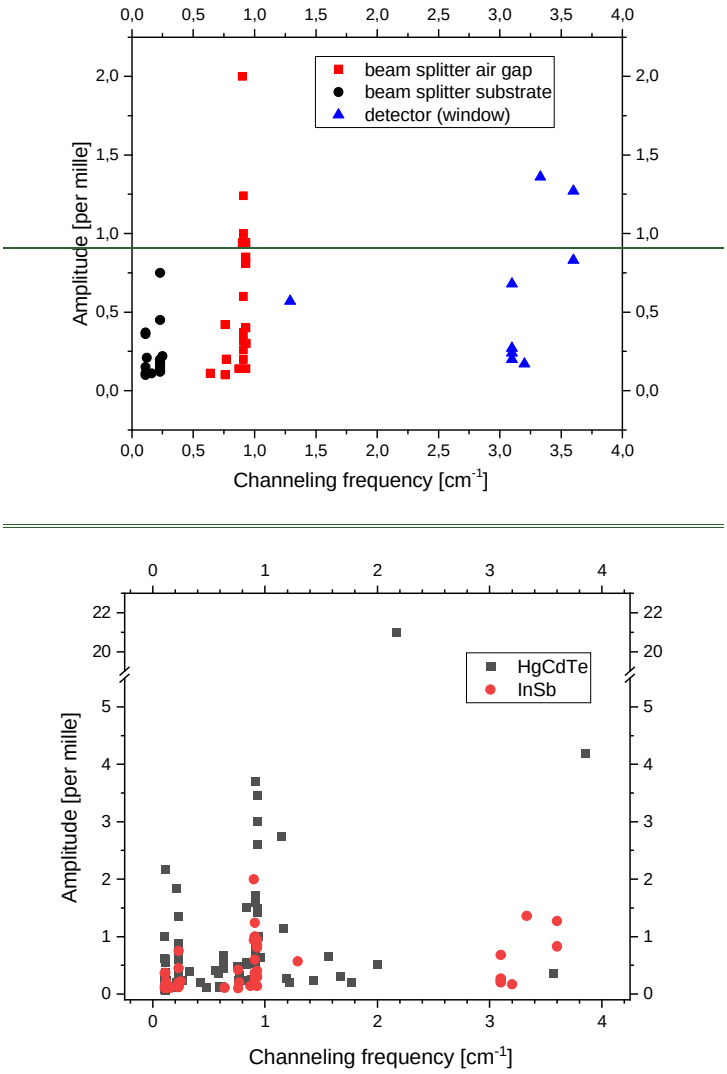

Figure 34: Amplitude of channeling frequencies as observed in InSb and HgCdTe test spectra ~~using NDACC filter no. 3.~~

~~Figure 4 shows the amplitude of the strongest channeling frequency of each spectrometer. In most cases, channeling caused by the gap of the beam splitter is the most pronounced one. The amplitudes range from 0.1 to 2.0 ‰ with a mean of (0.68 +/- 0.48) ‰ and a median of 0.60 ‰. These mean and median are consistent with the PROFFIT error estimate of 0.5 ‰ as used in Vigouroux et al. (2018). However, the channeling amplitude differs strongly from spectrometer to spectrometer and a few spectrometers show an amplitude of up to 2 ‰.~~

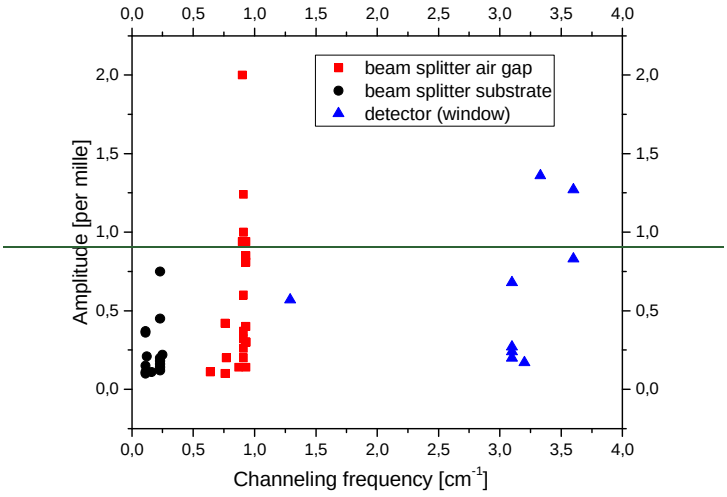

~~**Figure 3:** Amplitude of channeling frequencies as observed in InSb test spectra using NDACC filter no. 3.~~

Table ~~3~~4: Leading channeling frequencies F and their amplitudes A in the InSb detector regime. Channeling amplitudes larger than 0.6 ‰ are highlighted in bold.

FTIR site	**F 1 [cm^{-1}]**	**A 1 [‰]**	**F 2 [cm^{-1}]**	**A 2 [‰]**	**F 3 [cm^{-1}]**	**A 3 [‰]**	**F 4 [cm^{-1}]**	**A 4 [‰]**
Eureka	0.93	0.14	0.23	0.05	0.11	0.004		
Ny-Ålesund	**0.90**	**2.0**	0.11	0.08				
Thule	**0.91**	**1.0**	0.23	0.18	0.11	0.15	3.1	0.27
Kiruna	0.85	0.05	0.11	0.003	0.76	0.1		
Sodankylä	0.93	0.3	0.12	0.03	0.11	0.024	0.25	0.01
Harestua	0.91	0.37	0.10	0.02	**3.33**	**1.36**		
St. Petersburg	0.93	0.3	0.23	0.12	0.16	0.11	0.77	0.20
Bremen	0.93	0.3	0.23	0.16	0.11	0.05		
Karlsruhe	0.87	0.14			1.29	0.57		
Paris	0.91	0.2	0.25	0.05				
Garmisch	0.91	0.6	0.10	<0.1	3.1	0.24		
Zugspitze	0.91	0.26	0.11	0.025	0.10	0.035		
Jungfraujoch	**0.91**	**1.24**	0.23	0.08	0.12	0.02		

Toronto	**3.10**	**0.68**	0.21	0.05	0.11	0.02		
Rikubetsu	**0.90**	**0.94**	0.25	0.22	0.11	0.11	3.2	0.17
Boulder	**0.93**	**0.81**	**0.23**	**0.75**	0.11	0.11	3.6	0.83
Tsukuba	**0.93**	**0.94**	0.12	0.21	0.11	0.10		
Izaña – 2018	0.76	0.42	0.10	0.09	0.11	0.06	**3.6**	**1.27**
Izaña – 2019	0.83	0.07	0.10	0.02	0.11	0.03	3.1	0.20
Mauna Loa	**0.93**	**0.85**	0.23	0.45	0.11	0.36		
Altzomoni	0.64	0.11	1.82	0.04	0.74	0.03		
Wollongong	0.93	0.40	0.23	0.20	0.11	0.03		
Lauder ~~HR~~120HR	0.91	0.32	0.23	0.08	0.11	0.02		
Lauder ~~HR~~125HR	**0.91**	**1.0**	0.23	0.14	0.11	0.37	0.10	0.06
Arrival Heights	**0.91**	**0.94**	0.23	0.03	0.12	0.11	0.10	0.09

780 **Table ~~4~~5:** Leading channeling frequencies F and their amplitudes A in the HgCdTe detector regime. Channeling amplitudes larger than 1.~~0~~2 ‰ are printed in bold.

FTIR site	**F 1 [cm^{-1}]**	**A 1 [‰]**	**F 2 [cm^{-1}]**	**A 2 [‰]**	**F 3 [cm^{-1}]**	**A 3 [‰]**	**F 4 [cm^{-1}]**	**A 4 [‰]**
Eureka	**0.93**	**1.5**	0.23	0.2	0.11 0.10	0.14 0.05		
Ny-Ålesund	**0.91**	**1.6**	0.23 **0.21**	0.89 **1.85**	0.11 0.10	0.60 0.62	**2.17**	**21**
Kiruna	0.77	0.32	0.59	0.12	0.11	0.07		
Harestua	**0.91**	**3.7**	0.23 0.11	0.73 0.16	1.56 0.58	0.66 0.36	**3.85**	**4.2**
St. Petersburg	0.94	1.0	0.23 0.33	0.30 0.40	2.0 1.77	0.52 0.20		
Bremen	**0.93** 0.83	**1.43** 0.52	0.23	0.34	0.11 0.10	0.22 0.08		
Paris	0.83	0.56	0.26 0.23	0.23 0.37	0.21 0.12	0.13 0.23		
Zugspitze	0.91	0.79	0.23	0.25	0.11 0.10	0.18 0.19	3.57	0.36
Jungfraujoch	0.91	0.53	0.23 0.21	0.60 0.12	0.11 0.10	0.17 0.06		
Toronto	0.96 0.48	0.64 0.12	0.21	0.20	0.10	0.10		

Rikubetsu	**0.93** **0.83**	**1.44** **1.51**	0.23 0.18	0.62 0.14	**0.11** 0.10	**2.18** 1.01	0.42	0.21
Tsukuba	**0.93**	**3.46**	0.23	0.67	0.11 0.10	0.38 0.33	1.19	0.27
Izaña – 2018	0.76	0.23	0.63 0.56	0.45 0.41	0.11 0.10	0.13 0.13		
Izaña – 2019	0.75	0.48	0.63	0.54	0.11	0.17		
Mauna Loa	**0.93**	**2.60**	**0.23**	**1.35**	0.11 0.10	0.56 0.10	0.61	0.14
Altzomoni	0.88 0.63	0.25 0.68	1.67 1.43	0.31 0.23	0.11	0.08	1.22	0.21
Wollongong	**0.93** 0.82	**3.00** 0.23	0.23 0.59	0.25 0.13	0.11	0.16		
Lauder ~~HR~~120HR	0.91 ~~1.51~~	0.72 ~~0.08~~	0.23	0.06	0.11 0.10	0.12 0.07	1.51	0.08
Lauder ~~HR~~125HR	**0.91** ~~**1.14**~~	**1.69** ~~**2.74**~~	0.23	0.41	0.11 0.10	0.23 0.11	**1.14**	**2.74**
Arrival Heights	**0.91** ~~**1.16**~~	**1.72** ~~**1.15**~~	0.23	0.18	0.11 0.10	0.12 0.17	1.16	1.15

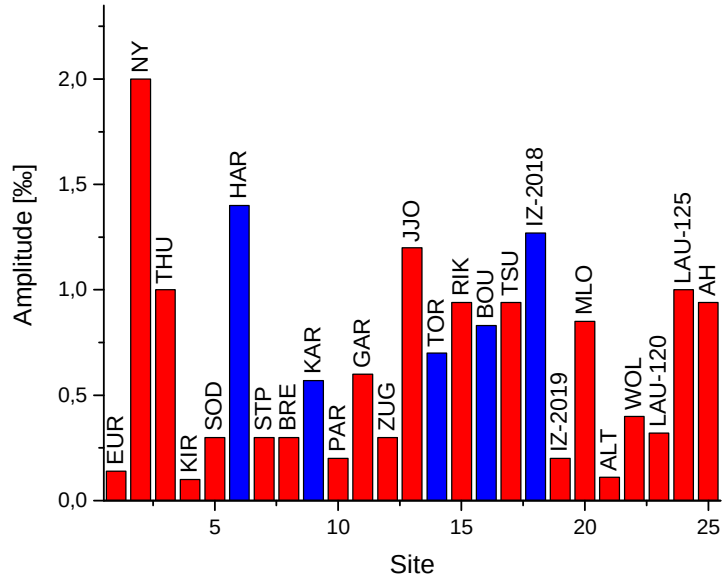

Figure 45: Amplitude of largest channeling fringe in test spectrum using InSb detector and NDACC filter number 3. Red bars indicate channeling due to beam splitter air gap and blue bars indicate detector window as source of channeling.

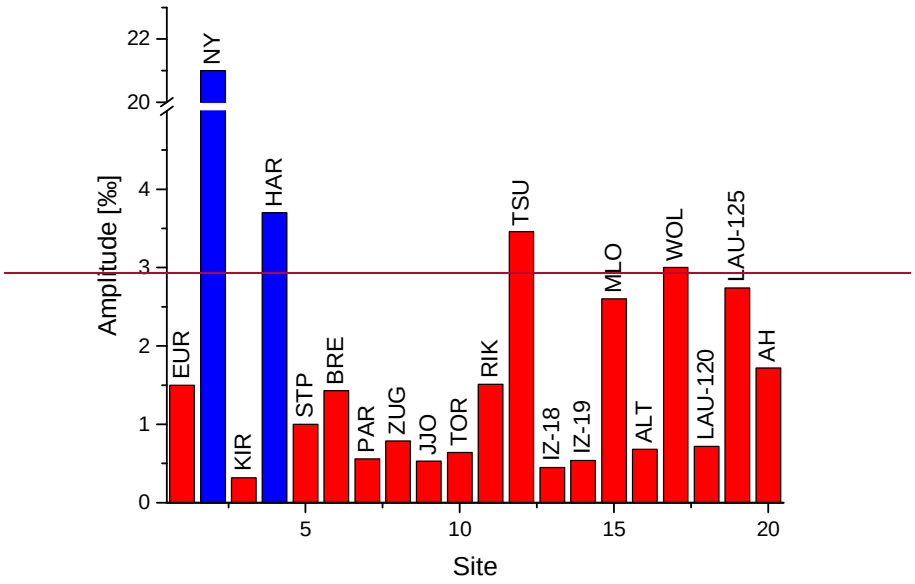

785

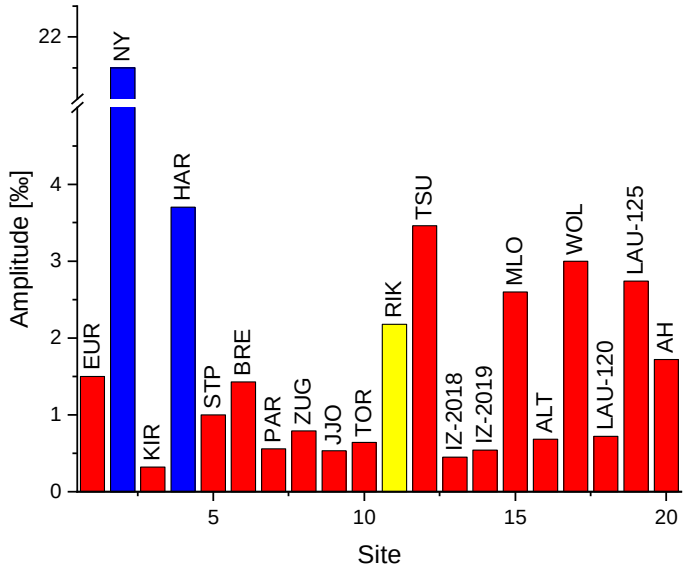

Figure ~~6~~5: Amplitude of largest channeling fringe in HgCdTe test spectrum. Red bars indicate channeling due to beam splitter air gap, yellow bar indicates beam splitter substrate and blue bars indicate detector window as source of channeling.

Figure 5 shows the amplitude of the strongest channeling frequency of each spectrometer. The amplitudes range from 0.1 to 2.0 ‰ with a mean of (0.68 +/- 0.48) ‰ and a median of 0.60 ‰. In most cases, channeling caused by the gap of the beam splitter is the most pronounced one. These mean and median are consistent with the PROFFIT error estimate of 0.5 ‰ as used in Vigouroux et al. (2018). However, the channeling amplitude differs strongly from spectrometer to spectrometer and a few spectrometers show an amplitude of up to 21 ‰.

4.2 HgCdTe detector domain

Fig. 4 and Table ~~4~~5 presents ~~lists~~ major channeling frequencies and their amplitudes in spectra recorded with an HgCdTe detector at about 1000 cm^{-1}. As for the InSb detector, most spectrometers show two dominant channeling frequencies: about 0.9 cm^{-1} and 0.1 or 0.2 cm^{-1} caused by the beam splitter (Table 1). Two spectrometers (Ny--Ålesund and Harestua) show an additional channeling frequency of 2.17 and 3.85 cm^{-1}, indicating that the wedge of the detector window is not sufficient in these cases.

Figure ~~5~~6 shows the amplitude of the strongest channeling frequency of each spectrometer. ~~In most cases, channeling caused by the gap of the beam splitter is the most pronounced one.~~ The amplitudes range from 0.3 to 21 ‰ with a mean of (2.45 +/- 4.50) ‰ and a median of 1.2 ‰. In most cases, channeling caused by the gap of the beam splitter is the most pronounced one. The amplitude is even larger as compared to the InSb domain that confirms that the wedge is more efficient in reducing the channeling at shorter wavelengths as calculated in Sect. 2. At several sites, a reduction of channeling amplitudes would be desirable in order to improve trace gas retrievals of species with weak signatures, in particular from HgCdTe spectra, e.g. of $ClONO_2$, HNO_3 or SF_6.

As for the InSb domain, channeling amplitudes differ strongly from spectrometer to spectrometer. Figure 7~~6~~ shows HgCdTe spectra with different levels of channeling of the same frequency (about 0.9 cm^{-1}) demonstrating the need of increasing the wedge of the gap and for narrowing the tolerances of wedges in the manufacturing of the beam splitters.

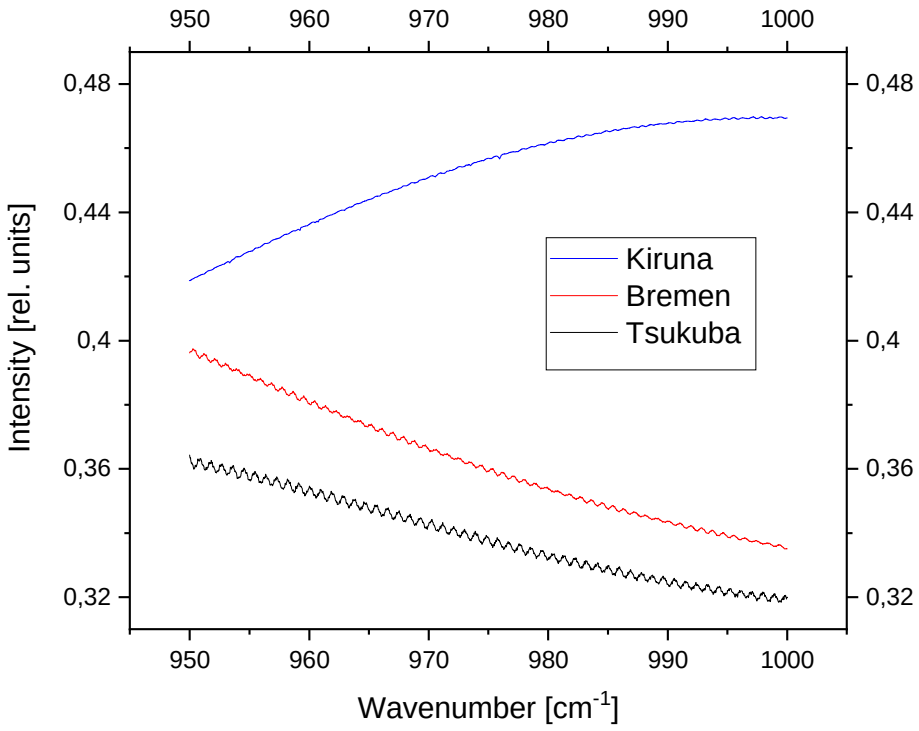
950
960
970
980
990
1000
0,48
0,44
0,4
0,36
0,32
Intensity [rel. units]
Kiruna
Bremen
Tsukuba
Wavenumber [cm-1]

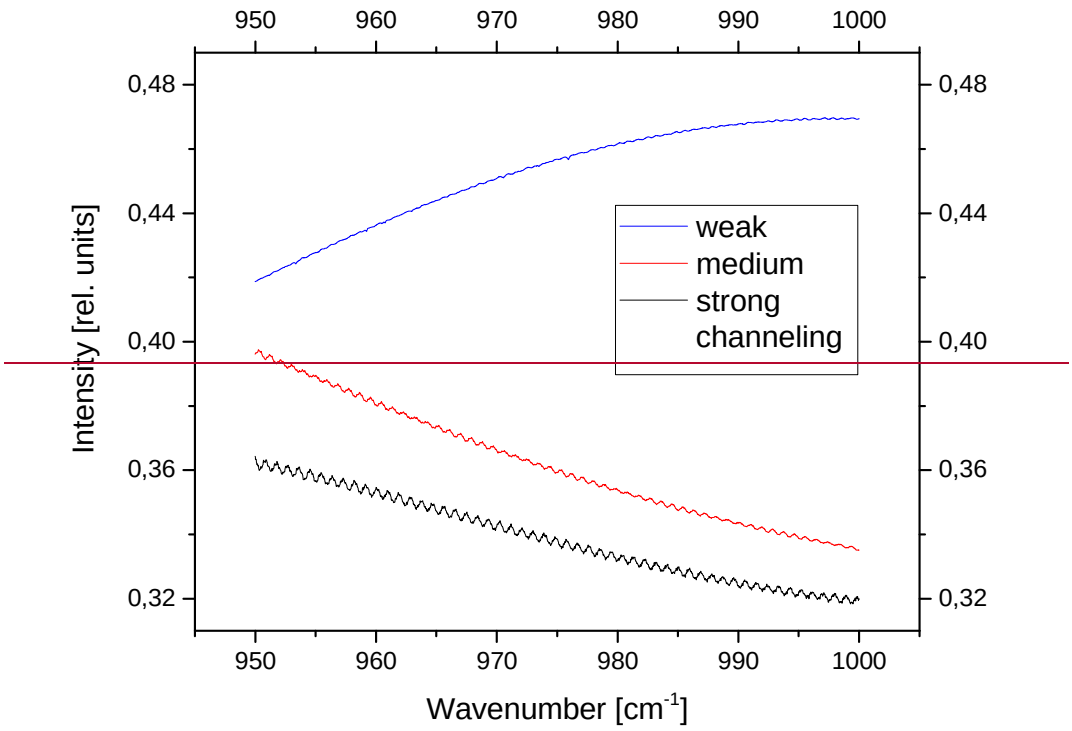

Figure ~~6~~7: HgCdTe spectra with low (0.32 ‰), medium (1.43 ‰) and high (3.46 ‰) channeling amplitude at 0.9 cm^{-1} frequency.

5 Investigation of a modified beam splitter design for reducing channeling

This test exercise has found that the channeling amplitude differs strongly from spectrometer to spectrometer. A few spectrometers (at Altzomoni, Izaña, Karlsruhe and Kiruna) use customer-specific beam splitters with an increased wedge of 1.75° for the air gap and 0.17°~~10 arc min~~ for the CaF_2 substrate and 0.13°~~8 arc min~~ for the KBr substrate. Their channeling amplitudes are the lowest among all the spectrometers studied in this paper. Unfortunately, this type of beam splitter is not a standard device and is not compatible with standard beam splitters, as it requires a realignment of the interferometer. Namely due to its incompatibility with unwedged far-infrared pellicle beam splitters, the manufacturer Bruker adheres to the standard design with lower substrate wedge.

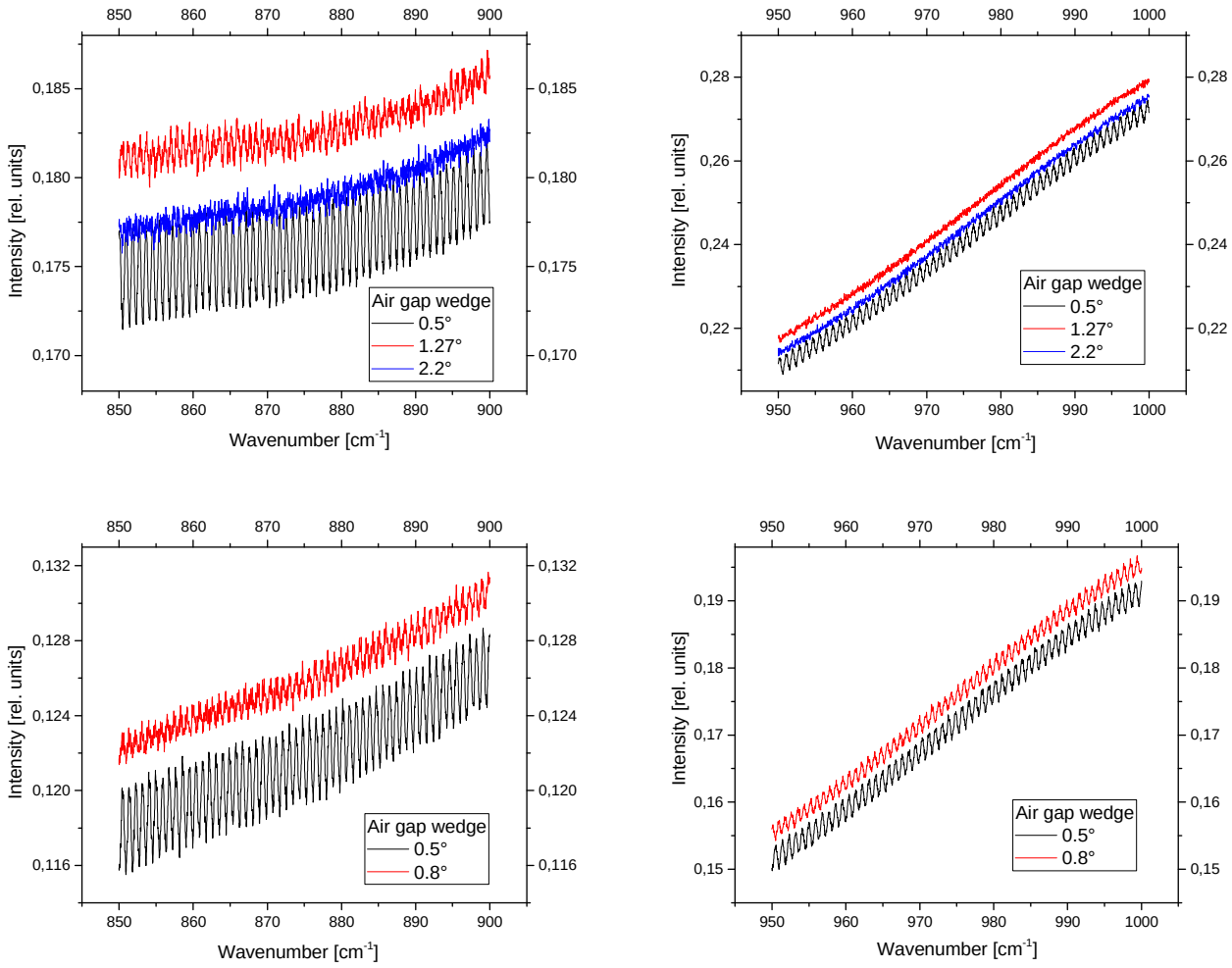

Figure 8~~7~~: HgCdTe spectra recorded with different wedges of the air gap in between beam splitter and compensator plate for the 850 to 950 cm^{-1} and the 950 to 1000 cm^{-1} spectral ranges. These measurements were made at Bruker Company, Ettlingen, using the same instrument.

To avoid the need for strongly wedged substrates, a different approach is proposed here. We focus on the wedge of the gap between the beam splitter and the compensator plate. Since the largest channeling amplitude (at 0.9 cm^{-1} frequency) is caused by the air gap, an increased wedge of this gap has the potential to reduce channeling significantly. The typical air gap wedge for the Bruker beam splitter is 0.5°. Different spacers with wedges of 0.5°, 1.27° and 2.2° have been manufactured by Bruker and tested. Figure 8~~7~~ (upper panels) shows the resulting channeling test spectra recorded with an HgCdTe detector. Similar to most of the NDACC spectrometers, the spectrum of the 0.5° wedged beam splitter shows a pronounced channeling with an

amplitude of 5.7 ‰. In contrast, the 1.27° and 2.2° wedged beam splitters are (nearly) free of channeling with an amplitude of 0.46 and of 0.87 ‰, respectively, that is close to the noise level of these spectra . Analysed in the 850 to 900 cm^{-1} spectral range, the amplitude is 8.9, 3.3 and 0.6 ‰ for a wedge of 0.5°, 1.27° and 2.2°, respectively. For InSb spectra, the 0.9 cm^{-1} channeling generates amplitudes of 0.9, 0.45 and 0.19 ‰ for beam splitters with wedges of 0.5°, 1.27° and 2.2°, respectively. To ensure compatibility between different beam splitters, the wedge should be limited to 0.8°. This design will be implemented in future Bruker HR spectrometers. Figure 8~~7~~ (lower panels) presents test spectra with an air gap wedge of 0.5° and 0.8°. In the 850 to 900 cm^{-1} spectral range, even the slightly increased wedge reduces the channeling by nearly 50 % (from 10 ‰ to 6 ‰). In the 950 to 1000 cm^{-1} range, however, the effect is smaller. Although the same spectrometer and beam splitter was used in the right and left hand panel the channeling amplitudes as well as the reduction factor varies. This is due to wavelength dependent reflectivity of the beam splitter.

Moreover, this exercise demonstrates that a wedge of about 2° on the air gap eliminates channeling even without a larger wedge of the beam splitter substrate. However, such a spectrometer completely free of channeling would result in non-interchangeability~~incompatibility~~ with beam splitters having a smaller air gap wedge and therefore, the need to realign the spectrometer after a beam splitter exchange. Furthermore, when switching from small to large wedge two new matched beam splitters are needed since the KBr beam splitter does not transmit visible light and therefore a second one (normally CaF_2 or glass) is needed for the alignment procedure. Switching within this new pair of beam splitters is possible without realignment. The ILS of the spectrometers with such a pair of beam splitters is good.

6 Conclusions

Firstly, this paper documents the channeling amplitudes for nearly all of the FTIR spectrometers used in NDACC. Such a systematic performance analysis is needed for improving the trace gas retrievals and for calculating complete error budgets and ~~.~~also to improve the consistency and quality of the products across the NDACC network

Within NDACC, laboratory test spectra of about twenty spectrometers were recorded and analysed. The derived channeling amplitudes range from 0.1 to 2.0 ‰ and from 0.3 to 21 ‰ in the InSb and HgCdTe domains, respectively. These values are not negligible when constructing the error budget of minor trace gases. A reduction of the channeling amplitudes is highly desirable for the analysis of gases like $ClONO_2$, HNO_3, HCHO, and SF_6~~.~~ since these species typically absorb in the order of about 5 ‰ ($ClONO_2$, HCHO) to 50 ‰ (HNO_3) of the incoming infrared light in the center of the signature.

Secondly, this study shows the potential to reduce channeling in several spectrometers and to improve the homogeneity within the network. The channeling frequencies allow us to determine the responsible optical component. A few instruments show channeling with a frequency of a few wavenumbers due to insufficiently wedged detector windows. Switching the detector window or, more easily, the entire detector including dewar and detector window, will help reduce channeling in these cases. Finally, we found that most spectrometers show two dominant channeling frequencies with about 0.1 or 0.2 cm^{-1} and 0.9 cm^{-1} corresponding to beam splitter substrate and beam splitter air gap, respectively, the latter usually dominant.. ~~In most cases, the channeling caused by the gap of the beam splitter is the leading one.~~ The option of reducing this channeling contribution was

investigated by adjusting the wedge angles on a test beam splitter. Increasing the wedge of this gap significantly reduces the channeling at 0.9 cm^{-1} and therefore, such a beam splitter design offers the promise of further reducing channeling. As a result of this study, Bruker changed the standard air gap wedge of its beam splitters from 0.5° to 0.8°. Furthermore, beam splitters with a wedge of 2° are available on request. Switching to this modified beam splitter design would contribute to further homogenization of the spectrometers operated within NDACC.

Appendix A

Table A1: List of optical filters used in the IRWG (InfraRed Working Group) of NDACC.

Filter number	Spectral range [µm]	Spectral range [cm^{-1}]	Target species examples
1	2.2 - 2.6	3850 - 4550	HF
2	2.6 - 3.3	3030 - 3850	HCN
3	3.2 - 4.1	2440 - 3130	HCl, CH_4, C_2H_6, HCHO, NO_2
4	3.9 - 5.0	2000 - 2560	N_2O
5	4.6 - 6.3	1590 – 2170	CO, NO, OCS
6	> 7.4	< 1350	O_3, $ClONO_2$, HNO_3, SF_6
7	9.8 – 13.0	770 - 1020	O_3, $ClONO_2$, HNO_3
8	7.5 – 10.2	980 - 1330	O_3

Data availability. Channeling test spectra used in this study are available on request from the corresponding author (thomas.blumenstock@kit.edu).

Author contributions. TB designed the study, performed the analysis, and wrote the paper. FH designed the analysis of the test spectra and wrote section 2 of the paper. AK improved the beam splitter and provided test spectra. All other authors did lab measurements and provided test spectra. All authors read and provided feedback on the paper.

Competing interests. The authors declare no competing interests.

Acknowledgements. We acknowledge Gerhard Kopp for stimulating discussions on Fabry Perot fringing effects. The authors like to acknowledge the project INMENSE (CGL2016-80688-P) funded by Ministerio de Economía y Competitividad from Spain. For the Altzomoni site UNAM (DGAPA grants IN111418 & IN107417), CONACYT (290589) and PASPA are acknowledged. The Paris site has received funding from Sorbonne Université, the French research center CNRS and the French

space agency CNES. Operations at Rikubetsu and Tsukuba sites are supported in part by the GOSAT series project. SPbU team was supported by Russian Foundation for Basic Research through the project no.18-05-00011. The Lauder and Arrival Heights FTIR measurements are core-funded by NIWA through New Zealand's Ministry of Business, Innovation and Employment Strategic Science Investment Fund. We also thank Antarctica New Zealand for providing support for the FTIR measurements at Arrival Heights, which includes test spectra collection. The Jungfraujoch FTIR experiment has received funding from the F.R.S. – FNRS, the Fédération Wallonie-Bruxelles, both in Brussels, Belgium, and from the GAW-CH programme of MeteoSwiss. ULiège acknowledges that the International Foundation High Altitude Research Stations Jungfraujoch and Gornergrat (HFSJG), 3012 Bern, Switzerland, made it possible to carry out our experiment at the Jungfraujoch Station. We like to thank the AWI Bremerhaven and the personnel at the AWIPEV station, Ny-Ålesund (Spitsbergen) for logistic and on-site support. Eureka measurements were made at the Polar Environment Atmospheric Research Laboratory (PEARL), primarily supported by the Natural Sciences and Engineering Research Council of Canada (NSERC), Environment and Climate Change Canada, and the Canadian Space Agency. Toronto measurements were made at the University of Toronto Atmospheric Observatory (TAO), primarily supported by NSERC and the University of Toronto. The National Center for Atmospheric Research is sponsored by the National Science Foundation. The NCAR FTS observation programs at Thule, GR, Mauna Loa, HI and Boulder, CO are supported under contract by the National Aeronautics and Space Administration (NASA). The FTIR stations Bremen, Garmisch, Izaña, Karlsruhe, and Ny-Ålesund have been supported ~~by~~ by ~~by~~ the German Bundesministerium für Wirtschaft und Energie (BMWi) via DLR under grants 50EE1711A-B&D. This work has been supported by the Federal Ministry of Education and Research (BMBF) Germany in the project TroStra (01LG1904A).

The article processing charges for this open-access publication were covered by a Research Centre of the Helmholtz Association.

References

Abrams, M. C., Toon, G. C., and Schindler, R. A.: Practical example of the correction of Fourier-transform spectra for detector nonlinearity, Applied Optics, 33, 6307-6314, doi:10.1364/AO.33.006307, https://www.osapublishing.org/ao/abstract.cfm?URI=ao-33-27-6307, 1994.

De Mazière, M., Thompson, A. M., Kurylo, M. J., Wild, J. D., Bernhard, G., Blumenstock, T., Braathen, G. O., Hannigan, J. W., Lambert, J.-C., Leblanc, T., McGee, T. J., Nedoluha, G., Petropavlovskikh, I., Seckmeyer, G., Simon, P. C., Steinbrecht, W., and Strahan, S. E.: The Network for the Detection of Atmospheric Composition Change (NDACC): history, status and perspectives, Atmos. Chem. Phys., 18, 4935-4964, https://doi.org/10.5194/acp-18-4935-2018, 2018.

Dohe, S., V. Sherlock, F. Hase, M. Gisi, J. Robinson, E. Sepúlveda, M. Schneider, and T. Blumenstock: A method to correct sampling ghosts in historic near-infrared Fourier Transform Spectrometer (FTS) measurements, Atmos. Meas. Tech., 6, 1981-1992, doi:10.5194/amt-6-1981-2013, 2013.

Gisi, M., F. Hase, S. Dohe, and T. Blumenstock: Camtracker: a new camera controlled high precision solar tracker system for FTIR-spectrometers, Atmos. Meas. Tech., 4, 47-54, 2011.

Hase, F., T. Blumenstock, C. Paton-Walsh: Analysis of the instrumental line shape of high-resolution Fourier transform IR spectrometers with gas cell measurements and new retrieval software, Appl. Opt. 38, 3417-3422, 1999

Hase, F., J.W. Hannigan, M.T. Coffey, A. Goldman, M. Höpfner, N.B. Jones, C.P. Rinsland, S.W. Wood: Intercomparison of retrieval codes used for the analysis of high-resolution, ground-based FTIR measurements, Journal of Quantitative Spectroscopy & Radiative Transfer 87, 25–52, 2004.

Hecht, E.: Optics, Fifth Edition, Pearson Education, ISBN 978013397726, p. 440, 2017.

Ismail, N., Calil Kores, C., Geskus, D., Pollnau, M.: The Fabry-Pérot resonator: Spectral line shapes, generic and related Airy distributions,linewidths, finesses, and performance at low or frequency-dependent reflectivity.OpticsExpress, 24(15): 16366-16389http://dx.doi.org/10.1364/OE.24.016366, 2016.

Keppel-Aleks, G., Toon, G.C., Wennberg, P.O., Deutscher, N.M.: Reducing the impact of source brightness fluctuations on spectra obtained by Fourier-transform spectrometry. Applied Optics. 46: 4774-9. PMID 17609726 DOI: 10.1364/AO.46.004774, 2007.

Messerschmidt, J., Macatangay, R., Notholt, J., Petri, C., Warneke,T., and Weinzierl, C.: Side by side measurements of CO_2 by ground-based Fourier transform spectrometry (FTS), Tellus B,62, 749–758,doi:10.1111/j.1600-0889.2010.00491.x, 2010.

Schneider, M. and F. Hase: Technical Note: Recipe for monitoring of total ozone with a precision of around 1 DU applying mid-infrared solar absorption spectra, ACP, Vol. 8, 63-71, SRef-ID: 1680-7324/acp/2008-8-63, 2008.

Vigouroux, C., Bauer Aquino, C. A., Bauwens, M., Becker, C., Blumenstock, T., De Mazière, M., García, O., Grutter, M., Guarin, C., Hannigan, J., Hase, F., Jones, N., Kivi, R., Koshelev, D., Langerock, B., Lutsch, E., Makarova, M., Metzger, J.-M., Müller, J.-F., Notholt, J., Ortega, I., Palm, M., Paton-Walsh, C., Poberovskii, A., Rettinger, M., Robinson, J., Smale, D., Stavrakou, T., Stremme, W., Strong, K., Sussmann, R., Té, Y., and Toon, G.: NDACC harmonized formaldehyde time series from 21 FTIR stations covering a wide range of column abundances, Atmos. Meas. Tech., 11, 5049-5073, https://doi.org/10.5194/amt-11-5049-2018, 2018.

Vigouroux, C., Langerock, B., Bauer Aquino, C. A., Blumenstock, T., Cheng, Z., De Mazière, M., De Smedt, I., Grutter, M., Hannigan, J., Jones, N., Kivi, Loyola, D., R., Lutsch, E., Mahieu, E., Makarova, M., Metzger, J.-M., Morino, I., Murata, I., Nagahama, T., Notholt, J., Ortega, I., Palm, M., Pinardi, G., Röhling, A., Smale, D., Stremme, W., Strong, K., Sussmann, R., Té, Y., van Roozendael, M., Wang, P., and Winkler, H.: TROPOMI/–Sentinel-5 Precursor formaldehyde validation using an extensive network of ground-based Fourier-transform infrared stations, Atmos. Meas. Tech., 13, 3751–3767, https://doi.org/10.5194/amt-13-3751-2020, 2020.

Wikipedia.org: https://en.wikipedia.org/wiki/Fabry-Perot_interferometer, last access on June 25, 2020; downloaded from Wikimedia Commons: https://commons.wikimedia.org.

Wunch, D., Toon, G. C., Wennberg, P. O., Wofsy, S. C., Stephens, B. B., Fischer, M. L., Uchino, O., Abshire, J. B., Bernath, P., Biraud, S. C., Blavier, J.-F. L., Boone, C., Bowman, K. P., Browell, E. V., Campos, T., Connor, B. J., Daube, B. C., Deutscher, N. M., Diao, M., Elkins, J. W., Gerbig, C., Gottlieb, E., Griffith, D. W. T., Hurst, D. F., Jiménez, R., Keppel-Aleks, G., Kort, E. A., Macatangay, R., Machida, T., Matsueda, H., Moore, F., Morino, I., Park, S., Robinson, J., Roehl, C. M., Sawa, Y., Sherlock, V., Sweeney, C., Tanaka, T., and Zondlo, M. A.: Calibration of the Total Carbon Column Observing Network using aircraft profile data, Atmos. Meas. Tech., 3, 1351–1362, https://doi.org/10.5194/amt-3-1351-2010, 2010.